MCB
Journals.ASM.org

Functional Redundancy of Sos1 and Sos2 for Lymphopoiesis and Organismal Homeostasis and Survival

Fernando C. Baltanás,[a] Martín Pérez-Andrés,[b] Alicia Ginel-Picardo,[a] David Diaz,[c] David Jimeno,[a] Pilar Liceras-Boillos,[a] Robert L. Kortum,[d] Lawrence E. Samelson,[d] Alberto Orfao,[b] Eugenio Santos[a]

Centro de Investigación del Cáncer, Instituto de Biología Molecular y Celular del Cáncer (CSIC-Universidad de Salamanca) Lab 1, Salamanca, Spain[a]; Centro de Investigación del Cáncer, Instituto de Biología Molecular y Celular del Cáncer (CSIC-Universidad de Salamanca) Lab 11, Salamanca, Spain[b]; INCYL, Universidad de Salamanca, Salamanca, Spain[c]; Laboratory of Cellular and Molecular Biology, National Cancer Institute, Bethesda, Maryland, USA[d]

Sos1 and Sos2 are ubiquitously expressed, universal Ras guanine nucleotide exchange factors (Ras-GEFs) acting in multiple signal transduction pathways activated by upstream cellular kinases. The embryonic lethality of Sos1 null mutants has hampered ascertaining the specific *in vivo* contributions of Sos1 and Sos2 to processes controlling adult organism survival or development of hematopoietic and nonhematopoietic organs, tissues, and cell lineages. Here, we generated a tamoxifen-inducible Sos1-null mouse strain allowing analysis of the combined disruption of Sos1 and Sos2 (Sos1/2) during adulthood. Sos1/2 double-knockout (DKO) animals died precipitously, whereas individual Sos1 and Sos2 knockout (KO) mice were perfectly viable. A reduced percentage of total bone marrow precursors occurred in single-KO animals, but a dramatic depletion of B-cell progenitors was specifically detected in Sos1/2 DKO mice. We also confirmed a dominant role of Sos1 over Sos2 in early thymocyte maturation, with almost complete thymus disappearance and dramatically higher reduction of absolute thymocyte counts in Sos1/2 DKO animals. Absolute counts of mature B and T cells in spleen and peripheral blood were unchanged in single-KO mutants, while significantly reduced in Sos1/2 DKO mice. Our data demonstrate functional redundancy between Sos1 and Sos2 for homeostasis and survival of the full organism and for development and maturation of T and B lymphocytes.

Ras proteins are critical signal transduction regulators which control cell proliferation, differentiation, and survival. These small GTPases are continuously cycling between inactive (Ras-GDP) and active (Ras-GTP) conformations in a process modulated by both negative (i.e., GTPase-activating protein [Ras-GAP]) and positive (i.e., guanine nucleotide exchange factor [Ras-GEF]) cell regulators. Among the Ras-GEF families identified in mammals, the Sos proteins are the most widely expressed and functionally relevant for Ras activation by upstream cellular signals (1, 2, 3, 4, 5).

The Sos family of Ras-GEFs encompasses two highly homologous members, Sos1 and Sos2 (Sos1/2), which are ubiquitously expressed and function in multiple signaling pathways promoting Ras activation downstream of a wide variety of tyrosine kinase receptors, as well as some cytokine and G protein-coupled receptors (4). Despite their structural homology, the functional properties of Sos1 and Sos2 appear to be markedly different. Prior analyses of constitutive knockout (KO) strains showed that Sos1 constitutive null animals die during midembryonic gestation (6), whereas adult Sos2 knockout mice are perfectly viable and fertile (7). The characterization of isolated Sos1 and Sos2 KO mouse embryonic fibroblasts also revealed a critical requirement for Sos1 but not Sos2 for transformation by upstream tyrosine kinases and for maintenance of long-term Ras–mitogen-activated protein kinase (Ras-MAPK) activation (6). The generation of conditional Sos1 null mutants (8) makes it now possible to address previously unanswered questions regarding the viability of adult mice following systemic deletion of Sos1 and the functional specificity versus redundancy of Sos1 and Sos2 in specific cell lineages and tissues.

Depending on the cellular context, Ras-mediated signaling controls a wide variety of biological, developmental, and oncogenic processes (9). In hematopoietic cells, activated Ras proteins are known to play a critical role in lymphocyte signaling processes involved in various T- and B-cell maturation steps (10, 11, 12, 13). Regarding B-cell development, various lines of experimental evidence suggest that Sos proteins, together with Ras guanyl nucleotide-releasing protein (RasGRP), play significant roles in Ras-mediated signaling downstream of epidermal growth factor receptor (EGFR) and B-cell receptor (BCR) stimulation (12, 14, 15). Maturation of thymocytes has also been shown to involve the participation of Ras signaling pathways through the coordinated contribution of different Ras-GEFs such as Sos1 and RasGRP1 (8, 12, 14, 16, 17). In this context, it has been suggested that Sos upregulation resulted in elevated risk of developing hematological malignancies, especially juvenile myelomonocytic leukemia (4, 18, 19). Altogether, these observations support a critical role for Sos family members during lymphocyte maturation in the thymus and the spleen and warrant further analysis of the specific contribution of Sos1 or Sos2 to these developmental processes.

Here, we evaluate the functional significance of Sos1 and Sos2 in a genetically modified mouse model which is able to bypass the known embryonic lethality of homozygous Sos1 null mutant mice (6). To this end, a floxed Sos1 allele (8) was placed under the control of a tamoxifen (TAM)-inducible Cre in order to try and achieve systemic, full-body deletion of the targeted Sos1 gene. This conditional Sos1 knockout mouse strain was then bred to constitutive Sos2 KO mice to generate experimental sets of wild-

Received 7 August 2013 **Returned for modification** 10 September 2013
Accepted 12 September 2013
Published ahead of print 16 September 2013
Address correspondence to Eugenio Santos, esantos@usal.es.

doi:10.1128/MCB.01026-13

type (WT), Sos1 and Sos2 single-KO, and Sos1/2 double-KO (DKO) animals. Despite the embryonic lethality of constitutive Sos1 KO mice, adult animals expressing the conditionally floxed Sos1 gene were fully viable, whereas absence of both Sos isoforms caused precipitous death in the Sos1/2 DKO mutants associated with marked reduction in lymphopoiesis, indicating that expression of either Sos1 or Sos2 alone is required and sufficient to support full viability of adult mice and that the Sos1 and -2 isoforms play essential, redundant but also distinct roles in controlling the development and homeostasis of the T- and B-cell lineages.

MATERIALS AND METHODS

Generation of tamoxifen-inducible, Sos1 null mutant mice. A mouse strain harboring a floxed version of Sos1 with exon 10 flanked by LoxP sites ($Sos1^{fl/fl}$) (8) was crossed with mice expressing a TAM-inducible Cre recombinase downstream of the RERT (Jackson Laboratories; stock number 017585, expressing an inducible Cre-^{ERT2}, Cre recombinase fused to a triple mutant form of the human estrogen receptor, from the endogenous Polr2a locus) promoter to generate homozygous $Sos1^{fl\text{-}Cre}/Sos1^{fl\text{-}Cre}$ mice that were then mated with constitutive Sos2 null mutant mice ($Sos2^{-/-}$) (7). Resulting heterozygous $Sos1^{fl\text{-}Cre/+}/Sos2^{+/-}$ mice were subsequently interbred to generate four distinct genotypes, analyzed in this report: control ($Sos1^{+\text{-}Cre/+\text{-}Cre}/Sos2^{+/+}$), Sos1 single-KO ($Sos1^{fl\text{-}Cre}/Sos1^{fl\text{-}Cre}$), Sos2 single-KO ($Sos1^{+\text{-}Cre/+\text{-}Cre}/Sos2^{-/-}$), and Sos1/2 DKO ($Sos1^{fl\text{-}Cre/fl\text{-}Cre}/Sos2^{-/-}$) (see Fig. 1A). All experimental groups were treated with TAM (after weaning the litters) under identical conditions to exclude any possible off-target effects. As TAM is an antagonist of the estrogen receptor, a 10-day washout period habituation with a soy-free diet (Teklad 16% global protein rodent diet, catalog no. 2916; Harlan) was given to the animals prior to the actual TAM treatments. Afterwards, a TAM-containing chow diet (Harlan; Teklad CRD TAM400/CreER) was administered, and experimental determinations were performed on each specific set of control and KO animals at various time points, most frequently at days +6 (6 days after initiating TAM treatment), +9, and +12. TAM treatment for shorter periods (4 days) triggered systemic, whole-body Cre recombinase activation and progressive removal of floxed Sos1 exon 10, which was 100% completed after 12 days, as detected by PCR assays with specific primers (see Fig. 1B) or Western immunoblots with specific antibodies (see Fig. 1C). For genotyping, DNA from mouse tails was investigated by PCR using specific primers to detect Sos1 or Sos2 deletion (7, 8). The animals were kept, handled, and sacrificed in accordance with current European and Spanish legislation, and all experiments were approved by the Bioethics Committee of our Cancer Research Center.

Phenotypic examinations. The Hemavet 950 instrument (Drew Scientific, Dallas, TX) was used to determine a wide range of hematological cell counts and other parameters in peripheral blood (PB) samples obtained from defined experimental groups of male mice treated with TAM for 12 days. Various biochemical parameters in blood serum from different experimental groups of animals treated with TAM for 14 days were also determined using reagent strips (total bilirubin, Panel-2, Panel-V, and Heart-2 test strips; Menarini Diagnostics, Barcelona, Spain) quantified on the Spotchem EZ 4430 instrument (Menarini Diagnostics).

Histological analyses. For histological examination, mice were perfused with a fixative solution as described elsewhere (20). The tissues of interest were dissected, postfixed for 2 h, and washed in phosphate buffer. Tissue blocks were then dehydrated and paraffin embedded. Paraffin sections (3 μm thick) were mounted on Superfrost-Plus slides (Thermo Scientific, Limburg, Germany) and deparaffinized with xylene, followed by decreasing concentrations of ethanol and distilled water. Hematoxylin-eosin (H&E) staining and the terminal deoxynucleotidyltransferase-mediated dUTP-biotin nick end labeling (TUNEL) assay were performed using standard procedures.

Western immunoblotting studies. Protein lysates were prepared by sample homogenization in a lysis buffer as previously described (21). Overall, 30 μg of total protein per sample lane was applied to 10% polyacrylamide gels, resolved by SDS-PAGE, and electrophoretically transferred to polyvinylidene difluoride (PVDF) membranes. After being blocked with 5% nonfat milk for 45 min at room temperature, the membranes were incubated overnight with a mouse anti-Sos1 monoclonal antibody (clone 25/SOS1; Becton Dickinson Biosciences [BD], San Jose, CA) and rabbit anti-Sos2 polyclonal antibody (sc-258; Santa Cruz Biotechnology, Dallas, TX) at 4°C. The membranes were then rinsed in 0.5% phosphate-buffered saline (PBS)–Tween (3 times for 5 min each), and the corresponding secondary antibodies (dilution of 1:5,000) were applied at room temperature for 1 h. After being washed with 0.5% PBS-Tween, the membranes were resolved using the Odyssey instrument (LI-COR Biosciences, Bad Homburg, Germany).

TABLE 1 List of fluorochrome-conjugated monoclonal antibodies used in the present study for flow cytometry immunophenotyping

Antibody[a]	Clone	Source
Anti-CD3ε–PerCP–Cy5.5	145-2C11	BD[b]
Anti-CD4–APC–H7	GK1.5	BD
Anti-CD5–V450	53-7.3	BD
Anti-CD8a–PO	5H10	Invitrogen[c]
Anti-CD11b–PerCP–Cy5.5	M1/70	BD
Anti-CD19–APC–H7	1D3	BD
Anti-CD21/CD35–APC	7G6	BD
Anti-CD23–PE	B3B4	BD
Anti-CD24–FITC	M1/69	BD
Anti-CD25–PE–Cy7	PC61	BD
Anti-CD44–APC	IM7	BD
Anti-CD45R (B220)–PO	RA3-B62	Invitrogen
Anti-c-Kit (CD117)–APC	2B8	BD
Anti-IgD–V450	11-26c.2a	BD
Anti-IgM–PE–Cy7 clone	R6-60.2	BD
Anti-TCRβ chain–PE	H57-597	BD
Anti-TCRγδ–FITC	GL3	BioLegend[d]

[a] APC, allophycocyanin; PO, Pacific Orange; PE, phycoerythrin; FITC, fluorescein isothiocyanate.
[b] BD, Becton Dickinson Biosciences, San José, CA.
[c] Paisley, United Kingdom.
[d] San Diego, CA.

Flow cytometry immunophenotyping. PB and bone marrow (BM) samples as well as cell suspensions from fresh, mechanically disaggregated thymi and spleens of mice from all experimental groups were obtained. Briefly, 2×10^6 cells per sample were incubated in the dark for 30 min with specific mixtures of fluorochrome-conjugated antibodies (Table 1) recognizing specific cell populations of interest in the thymus, BM, spleen, and PB. Stained samples were then centrifuged ($250 \times g$, 5 min) and washed in 0.5 ml of PBS. Finally, 1×10^6 cells were acquired using the FACS Diva software (BD) in a FACSAria flow cytometer (BD). For data analysis, the Infinicyt software (Cytognos SL, Salamanca, Spain) was used.

Bone marrow transplantation. Four distinct experimental groups were examined: control mouse recipients receiving WT BM cells (control/control; $n = 7$); control mice receiving DKO BM cells (control/DKO; $n = 10$); DKO mice receiving control BM cells (DKO/control; $n = 7$), and DKO mice receiving DKO BM cells (DKO/DKO; $n = 7$). Procedures for BM transplantation were as previously described (22). Briefly, control or DKO BM cells were isolated from 6-week-old female donors by flushing tibias, femurs, and iliac crests with Dulbecco's modified Eagle medium (Invitrogen). Red blood cells were then lysed through incubation for 5 min in ice-cold ammonium chloride (140 mM in 17 mM Tris). After a double wash with PBS and mild centrifugation, 7.5×10^6 BM cells were injected intravenously into the tail veins of 20-day-old WT and DKO male mouse receptors. Recipient animals had been sublethally irradiated (7.5 Gy; Gammacell 1000 Elite with cesium 137 source operating at 243 cGy/min; Best Theratronics, Canada) to remove their own BM 24 h before

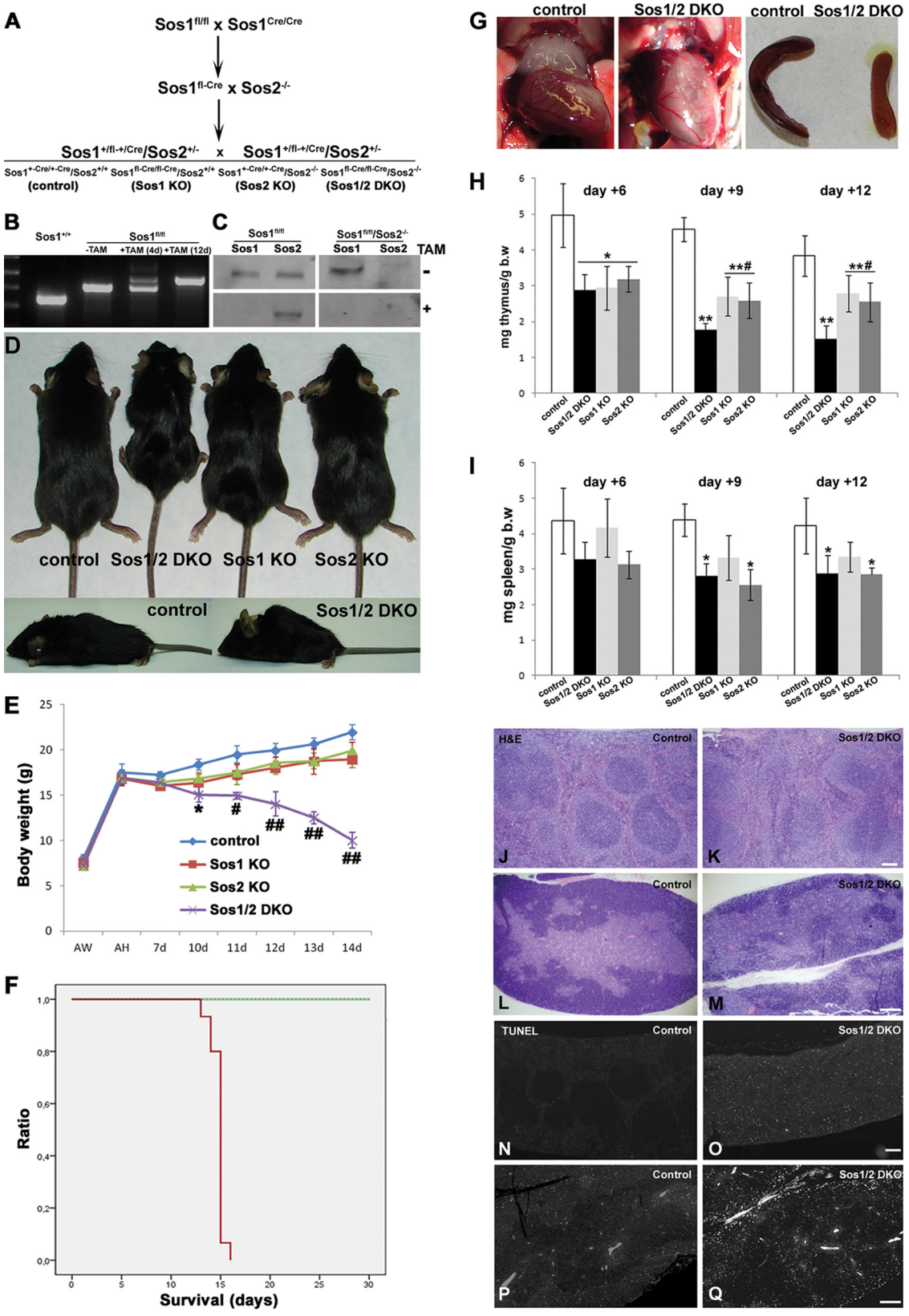

FIG 1 Generation and phenotypic characterization of single and double Sos null mutant mice. (A) Schematic outlining of the generation of Sos1 and -2 and Sos1/2 null mice. (B) PCR amplification of DNA extracted from the tails of control and Sos1$^{fl/fl}$ mice. Partial excision of Sos1 exon 10 was visible at day +4, and complete exon 10 removal was accomplished after 12 days of TAM treatment. (C) Western blot showing Sos1 depletion in isolated cells from Sos1 KO and Sos1/2 DKO mice before (−) or after (+) 12 days of TAM treatment. (D) Photographs of euthanized mice from all experimental groups. Control and Sos single-KO

TABLE 2 Hematological and biochemical parameters from peripheral blood and serum of control and Sos single and double null mutant mice

Parameter	Value[a] (mean ± SD) for group:			
	Control	Sos1/2 DKO	Sos1 KO	Sos2 KO
White blood cells/μl ($\times 10^3$)	4.8 ± 1.4	2 ± 0.5*	4.5 ± 1.3	3.3 ± 0.4
Neutrophils (%)	22 ± 4	29 ± 5	23 ± 5	25 ± 3
Lymphocytes (%)	70 ± 2	49 ± 4**	64 ± 7	63 ± 3
Monocytes (%)	7.7 ± 2.3	17.5 ± 3.7*	11.7 ± 3.6	10.5 ± 1.6
Eosinophils (%)	0.5 ± 0.4	4.9 ± 3.6*	1.4 ± 1	0.6 ± 0.5
Basophils (%)	0.08 ± 0.12	0.1 ± 0.08	0.25 ± 0.35	0.07 ± 0.08
Red blood cells/μl ($\times 10^6$)	8 ± 0.7	8.7 ± 0.2	8 ± 1	8.7 ± 0.5
Hemoglobin (g/dl)	13 ± 1	13 ± 0.5	14 ± 0.6	13.7 ± 0.6
Platelets/μl ($\times 10^3$)	907 ± 76	1,678 ± 178**	692 ± 163§	1,106 ± 167#
Total protein (g/dl)	5 ± 1	3.1 ± 0.7**	4.3 ± 0.4	4.5 ± 0.4
Albumin (g/dl)	2.4 ± 0.2	1.5 ± 0.3**	2.1 ± 0.3	2.3 ± 0.1
Alkaline phosphatase (IU/liter)	488 ± 80	201 ± 69**	622 ± 185	481 ± 54
Creatine phosphokinase (IU/liter)	781 ± 315	1,424 ± 533*	780 ± 293	772 ± 232
Glutamic-oxaloacetic transaminase (IU/liter)	76 ± 17	419 ± 194**	66 ± 15	57 ± 19
Glutamate pyruvate transaminase (IU/liter)	39 ± 8	254 ± 91**	29 ± 11	33 ± 12
Lactate dehydrogenase (IU/liter)	975 ± 335	2,116 ± 629**	986 ± 499	938 ± 357
Creatinin (mg/dl)	0.5 ± 0.1	0.2 ± 0.1**	0.5 ± 0.1	0.5 ± 0.1
Blood urea nitrogen (mg/dl)	23 ± 5	40 ± 13	27 ± 6	24 ± 6
Uric acid (mg/dl)	3.7 ± 0.7	2.5 ± 1.2	2.7 ± 1	2.3 ± 1
Triglyceride (mg/dl)	78 ± 16	76 ± 46	87 ± 17	93 ± 38
Cholesterol (mg/dl)	80 ± 10	72 ± 15	66 ± 18	77 ± 17
Glucose (mg/dl)	100 ± 27	151 ± 49	139 ± 17	134 ± 33
Calcium (mg/dl)	11 ± 1	10 ± 1	10 ± 1	10 ± 0.4

[a] Hematological parameters from peripheral blood were measured at day +12 of TAM treatment, while serum parameters were assessed at day +14 ($n = 6$ and 20 for hematological and biochemical studies, respectively). *, $P < 0.05$ for Sos1/2 DKO mice versus the rest of the groups; **, $P < 0.01$ for Sos1/2 DKO mice versus the rest of the groups; #, $P < 0.05$ for Sos2 KO mice versus Sos1 KO mice; §, $P < 0.05$ for Sos1 KO mice versus control mice.

grafting. Once transplanted, recipient animals were treated with a soy-free diet for 15 days, followed by 12 days of TAM administration through the diet. Nontransplanted, irradiated recipients were used as controls for successful irradiation. All irradiated nontransplanted mice died around 10 days after radiation.

Statistical methods. For all statistical analysis the SPSS v20 software package (SPSS Inc., Chicago, IL) was used. The Mann-Whitney U test was used to evaluate the statistical significance of differences among different animal groups. Survival curves were plotted according to the method of Kaplan and Meier and compared by the log rank test. *P* values ≤0.05 were considered statistically significant.

RESULTS

Simultaneous disruption of Sos1 and Sos2 causes adult lethality, whereas Sos1 or Sos2 single-knockout mice are viable. In order to test the viability of adult mice lacking Sos1, alone or combined with loss of Sos2, we produced a TAM-inducible, floxed Sos1 null mutant strain and crossed it with constitutive Sos2 KO mice. Analysis of the resulting live offspring after TAM treatment for disruption of the floxed Sos1 allele allowed recognition of four specific genotypes: wild type, Sos1 single-KO, Sos2 single-KO, and Sos1/2 DKO. These four genotypes were instrumental for ascertaining the functional specificity versus redundancy of the Sos1 and -2 isoforms as regards the sustainability of the viability and survival of the full organism and/or their impact on distinctive phenotypes in specific organs or cell lineages within these animals (Fig. 1A).

Overall, our results showed that single Sos1 deficiency alone during adulthood did not result in any obvious, external phenotypic alteration, as these animals showed full viability; similarly, the absence of Sos2 did not cause any observable alterations com-

mice displayed normal phenotype, while the TAM-treated Sos1/2 DKO mouse was undersized and exhibited hunching of the spine. (E) Body weight measurements at different stages, including after weaning (AW), after habituation diet (AH), and at various times (days 7 to 14) during TAM treatment. (F) Kaplan-Meier survival plot showing that single Sos1 or Sos2 disruption did not compromise mouse survival (green line) while Sos1/2 DKO mutants died 2 weeks after TAM induction (red line). (G) Photographs of thymi (left) and spleens (right) of WT and Sos1/2 DKO mice at day 14 after TAM induction. In Sos1/2 DKO mice, the thymus almost disappeared while the spleen was undersized versus WT controls. (H and I) Bar charts representing the ratios between the weights of the thymus or spleen per gram of total body weight (b.w) for all experimental mouse groups after 6, 9, and 12 days of TAM treatment. The weight of the thymus was significantly reduced in Sos-null mice at all periods of time examined versus controls (H). In addition, at days 9 and 12 after TAM treatment, the thymi of Sos1/2 DKO mice were diminished versus those of Sos single mutants (H). Data from the spleen revealed reduced weights in both Sos2 and double mutants with respect to controls (I). (J to M) Paraffin sections from spleens and thymi of control and Sos1/2 DKO mice at day 12 after TAM feeding, stained with hematoxylin and eosin (H&E). The histology of the spleen appeared altered, with highly disrupted germinal centers in the DKO mice (K). In the thymus, Sos1/2 DKO mice exhibited a marked reduction of the cortex (M). (N to Q) Terminal deoxynucleotidyltransferase-mediated dUTP-biotin nick end labeling (TUNEL) assays performed in paraffin sections from spleens and thymi of control and Sos1/2 DKO mice at day 12 after TAM treatment showed increased numbers of apoptotic cell bodies both in the spleens (O) and the thymi (Q) from Sos1/2 DKO mice versus WT controls (N and P). *, $P < 0.05$ versus control; **, $P < 0.01$ versus control mice; #, $P < 0.05$ versus the rest of the groups; ##, $P < 0.01$ versus the rest of the groups ($n = 25$ for all different genotypes analyzed). Bars, 1 mm.

TABLE 3 Distribution of the major subpopulations of BM cells in WT control and Sos null mutant mice

Cell type[a]	Genotype	Mean % ± SD[b] on TAM treatment day: +6	+9	+12
BM lymphocytes (FSC^{lo} SSC^{lo} $CD11b^-$ $CD117^-$ $TER119^-$)	Control	20 ± 4	22 ± 12	15 ± 2
	Sos1/2 DKO	19 ± 3	11 ± 3	12 ± 2
	Sos1 KO	17 ± 5	16 ± 4	14 ± 3
	Sos2 KO	23 ± 4	12 ± 5	16 ± 2
Granulomonocytic cells ($FSC^{int/hi}$ $SSC^{int/hi}$ $CD11b^+$ $CD117^-$ $TER119^-$)	Control	47 ± 11	40 ± 9	50 ± 12
	Sos1/2 DKO	30 ± 8*	27 ± 5*	23 ± 9*
	Sos1 KO	42 ± 12	36.4 ± 10	26 ± 7*
	Sos2 KO	39 ± 6	35 ± 9	29 ± 4*
BM erythroid cells (FSC^{lo} $SSC^{int/hi}$ $CD11b^-$ $CD117^-$ $TER119^+$)	Control	33 ± 8	38 ± 13	34 ± 10
	Sos1/2 DKO	51 ± 8*	62 ± 7*	58 ± 17*
	Sos1 KO	38 ± 11	48 ± 12#	59 ± 9*
	Sos2 KO	37 ± 8●	52 ± 11	49 ± 11*
BM progenitors ($FSC^{lo/int}$ $SSC^{lo/int}$ $CD11b^-$ $CD117^-$ $TER119^-$)	Control	3.7 ± 1	2 ± 1	3 ± 0.3
	Sos1/2 DKO	1.4 ± 0.3*	0.8 ± 0.2*	2 ± 0.9*
	Sos1 KO	1.9 ± 0.5*	1.3 ± 0.5*●	1.4 ± 0.2*
	Sos2 KO	1.9 ± 0.4*	1.3 ± 0.6*●	1.4 ± 0.4*

[a] FSC, forward light scatter; SSC, sideward light scatter; lo, low; hi, high; int, intermediate.
[b] *, $P < 0.05$ versus control; ●, $P < 0.05$ versus Sos1/2 DKO ($n = 5$ for control and Sos1 or Sos2 single-KO mice; $n = 7$ for Sos1/2 DKO mice).

pared to WT mice, as previously described (7). In contrast, combined disruption of Sos1 and Sos2 rapidly showed dramatic effects by strongly affecting the external phenotype of adult mice. Thus, Sos1/2 DKO mice showed dramatic body size reduction associated with an emaciated, runted appearance and had a markedly hunched upper back, limb weakness, and shaky body movements (Fig. 1D). Detailed body weight measurements (Fig. 1E) also revealed similar values for the WT, Sos1 single-KO, and Sos2 single-KO animals after 2 weeks of TAM induction. In contrast, the Sos1/2 DKO mice exhibited progressive body weight reduction, which was visible immediately after TAM administration had been started (Fig. 1D and E). This translated into a significantly compromised overall survival of the Sos1/2 DKO mice; all of them died around 2 weeks after TAM induction, whereas single disruption of the Sos1 or Sos2 isoforms did not affect viability in adult mice, even after very long periods of TAM induction (Fig. 1F). These results indicate that, despite the embryonic lethality of Sos1 null mice (6), depletion of Sos1 does not affect viability during adulthood and the remaining, resident Sos2 can substitute for Sos1 in those animals. However, concomitant deletion of both Sos isoforms is absolutely critical for adult mouse survival, indicating that expression of Sos1 or Sos2 alone is required and also sufficient for adult mouse viability.

Blood analysis of Sos1 or Sos2 single-KO animals did not show any significant alterations of various blood parameters, except for the platelet counts, which appeared to be significantly increased in Sos1/2 DKO mice versus both the WT and the single-Sos-deficient groups (Table 2). In addition, Sos2-deficient mice showed an increased total number of platelets versus Sos1 KO mice (Table 2). Conversely, combined disruption of Sos1 and Sos2 resulted in a >50% reduction in the white blood cell (WBC) count compared to WT controls ($P = 0.03$) (Table 2). Such reduced WBC counts were mostly due to a significant drop in the total number of lymphocytes to less than one-third of WT values ($P = 0.002$) (Table 1); the absolute counts of other WBC populations remained almost unaltered ($P > 0.05$) (Table 2).

Similar to blood cell counts, normal serum biochemical parameters were also found for mice with a single deficiency in Sos1 or Sos2 versus control WT mice, as they did not exhibit any abnormal values (Table 2). In contrast, Sos1/2 DKO mutants showed significantly reduced levels of total serum proteins and albumin, together with increased serum levels of lactate dehydrogenase (LDH), creatinine phosphokinase (CPK), and liver enzymes (e.g., alkaline phosphatase [ALP], glutamic pyruvic transaminase [GPT], and glutamic-oxaloacetic transaminase [GOT]), suggesting the occurrence of liver failure in these animals. Other biochemical parameters related to fatty acid or carbohydrate metabolism remained mostly unaltered in the Sos1/2 DKO mice (Table 2).

Necropsies performed after TAM induction in all experimental groups did not show any evident signs of gross internal organ alteration in the Sos1 or Sos2 null mutants (versus WT controls). Strikingly however, the Sos1/2 DKO mice showed a marked, progressive size reduction of both the thymus (this organ was almost gone) and spleen, compared to WT animals (Fig. 1G), in the absence of any visible morphological alteration (versus WT mice) of the hearts, lungs, kidneys, livers, or brains of these DKO animals.

Although other organ and tissue functions may also be affected, the above observations focused our initial studies on a more detailed examination of lymphoid organs (thymus and spleen) in our Sos KO animals. In this regard, we observed a significant weight reduction of the thymi extracted from both single and double Sos null mutants compared to WT controls, from day +6 of TAM treatment onwards. Of note, at days +9 and +12 of TAM feeding (when Sos1 deletion is complete), the weights of the thymi of Sos1/2 DKO mutants were significantly lower ($P = 0.008$) than those of similarly treated Sos1 or Sos2 single-KO mice (Fig. 1H). In turn, only the spleen weights of both Sos2 single-KO mice and Sos1/2 DKO mice showed statistically significant differences versus those of WT control mice after 9 and 12 days of TAM induction but not at day +6 (Fig. 1I).

Histological examination of the thymus and spleen did not

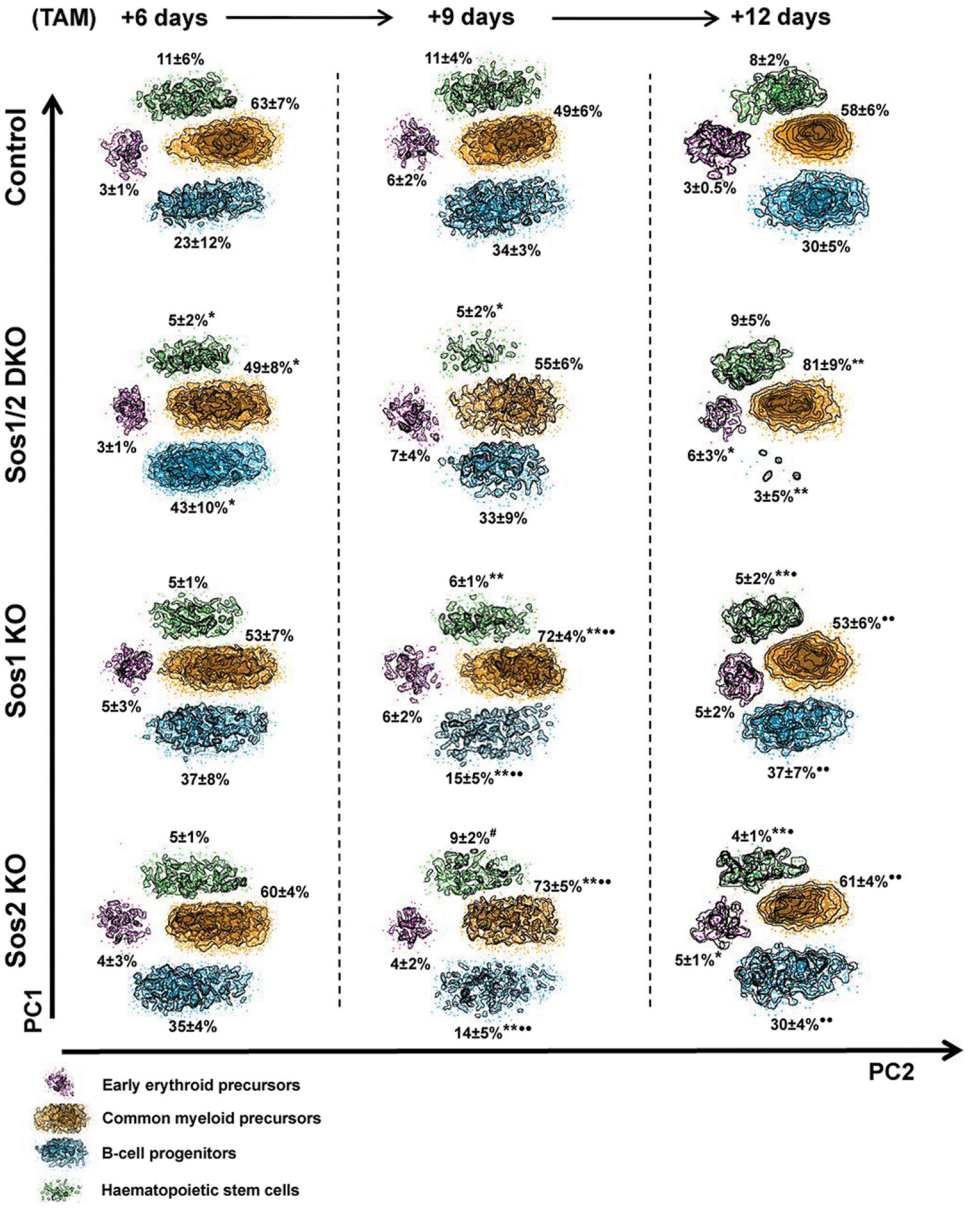

FIG 2 Bone marrow progenitor populations in Sos KO mice by analysis of single $Sca1^+$ and/or $CD117^+$ cells. Shown are representative density dot plots of BM progenitors including hematopoietic stem cells ($Sca1^+$ $CD117^+$ cells), common myeloid precursors ($Sca1^-$ $CD117^+$ $CD19^-$ $TER119^-$ cells), B-cell progenitors ($Sca1^-$ $CD117^+$ $CD19^+$ $TER119^-$ cells), and early erythroid precursors ($Sca1^-$ $CD117^+$ $CD19^-$ $TER119^+$ cells) from WT control mice and both double and single Sos mutants 6, 9, and 12 days after TAM feeding. The mean percentages ± standard deviations (SD) are shown for each cell population. Statistically significant differences are indicated as follows: *, $P < 0.05$ versus control mice; **, $P < 0.01$ versus control mice; ●, $P < 0.05$ versus Sos1/2 DKO mice; ●●, $P < 0.01$ versus Sos1/2 DKO mice; #, $P < 0.05$ versus Sos1 mice ($n = 5$ for control and Sos1 or Sos2 single KO mice; $n = 7$ for Sos1/2 DKO mice). PC1 and -2, principal components 1 and 2.

show any obvious abnormalities in the Sos1 or Sos2 single-KO animals versus WT controls but documented very significant morphological alterations in the same organs of the Sos1/2 DKO mice (Fig. 1J and M). In particular, H&E staining of paraffin sections showed a marked disruption of the germinal centers of the spleen (Fig. 1J versus K) and the cortex of the thymus (Fig. 1L versus M) of Sos1/2 DKO animals versus WT mouse organs. In addition, a marked enhancement of cell death was found both in the spleens and the thymi of the Sos1/2 DKO mutants by the TUNEL assay (Fig. 1N and Q). These findings, together with the remarkable drop of PB lymphocyte counts found in the Sos1/2 DKO animals, warranted further examination of the developmental process of T- and B-lymphocyte progenitors in the BM, as well as any possible alterations of their respective maturation processes in the thymus, spleen, and PB.

BM early progenitor cell populations are differentially affected in Sos1 or Sos2 single-KO mice versus Sos1/2 DKO mice. Multiparameter flow cytometry analysis of the distribution of different subpopulations of hematopoietic cells in the BM (23) of TAM-treated control and KO animals revealed significant changes among Sos1/2 DKO mice. These consisted of a significant relative decrease from day +6 onwards of $Sca1^+$ $CD117^+$ BM

TABLE 4 Distribution of the different maturation-associated B-cell subsets in the bone marrow of control and Sos mutant mice

Maturation stage	Group	Mean % ± SD[a] on TAM treatment day: +6	+9	+12
Pro-B cells ($CD117^+$ $Sca1^-$ $TER119^-$ $CD11b^-$ $CD19^+$ $B220^-$ IgM^-)	Control	5.6 ± 3.2	4.73 ± 0.7	7.7 ± 2
	Sos1/2 DKO	3.8 ± 0.4	5 ± 3.1	0.9 ± 1.3**
	Sos1 KO	5.6 ± 1.4	2.3 ± 1.7*	5.2 ± 1.2●●
	Sos2 KO	4 ± 1	2.7 ± 1.3*	3.4 ± 1.4●
Pre-B cells ($CD117^-$ $Sca1^-$ $TER119^-$ $CD11b^-$ $CD19^+$ $B220^-$ IgM^-)	Control	70 ± 6	59 ± 7	66 ± 4
	Sos1/2 DKO	70 ± 5	49 ± 9	27 ± 14**
	Sos1 KO	66 ± 7	59 ± 12	71 ± 5●●
	Sos2 KO	65 ± 3	58 ± 8	63 ± 16●●
Immature B cells ($CD117^-$ $Sca1^-$ $TER119^-$ $CD11b^-$ $CD19^+$ $B220^-$ IgM^+)	Control	18 ± 2	23 ± 3	18 ± 4
	Sos1/2 DKO	19 ± 3	24 ± 3	21 ± 8
	Sos1 KO	18 ± 2	20 ± 2	18 ± 3
	Sos2 KO	20 ± 2	22 ± 4	19 ± 3
Recirculating B lymphocytes ($CD117^-$ $Sca1^-$ $TER119^-$ $CD11b^-$ $CD19^+$ $B220^+$ IgM^+)	Control	7 ± 4	13 ± 5	9 ± 5
	Sos1/2 DKO	8 ± 3	22 ± 10	51 ± 19**
	Sos1 KO	11 ± 6	20 ± 14	6 ± 3●●
	Sos2 KO	11 ± 5	18 ± 5	15 ± 9●●

[a] Values correspond to the percentages of each cell subset from all $CD19^+$ BM B cells. *, $P < 0.05$ versus control; **, $P < 0.01$ versus control; ●, $P < 0.05$ versus Sos1/2 DKO; ●●, $P < 0.01$ versus Sos1/2 DKO ($n = 5$ for control and single Sos1 or Sos2 KO mice; $n = 7$ for Sos1/2 DKO mice).

progenitors and granulomonocytic cells at the expense of an increase of erythroid cells, with similar B-cell ($CD19^+$) numbers versus WT control animals (Table 3). Similar changes were also found after longer periods of TAM treatment in the BM of Sos1 or Sos2 single-KO mice (Table 3).

A more detailed analysis of early $Sca1^+$ $CD117^+$ BM precursors in control WT mice showed that they represented around 3 to 4% of the whole cellularity, independently of prolonged TAM treatment (Table 3). By contrast, both Sos1 or Sos2 single-KO and Sos1/2 DKO mice displayed a significantly marked reduction (>50%) of the size of this pool of early $Sca1^+$ $CD117^+$ progenitors versus WT animals (Table 3). In more detail, fluorescence-activated cell sorter (FACS) analysis revealed that, while the different subpopulations within this pool of early progenitors (e.g., $Sca1^-$ $CD117^+$ $CD19^-$ $TER119^-$ common myeloid precursors, $CD19^+$ B-lymphoid progenitors, $Sca1^+$ $CD117^+$ hematopoietic stem cells [HSC], and $TER119^+$ early erythroid precursors) were not affected by TAM treatment in control WT mice, they were variably impacted by the Sos1 and/or Sos2 protein deficiency (Fig. 2), the specific changes observed depending on the genotype and the duration of the TAM treatment period (Fig. 2). Accordingly, whereas the Sos1 and Sos2 single-KO mice exhibited rather parallel patterns of fluctuation in the percentage of each subpopulation of BM precursors at the times evaluated, the Sos1/2 DKO mice showed more-dramatic changes, which specifically targeted B-cell progenitors (Fig. 2). Indeed, at day +12 of TAM treatment, the percentage of $CD19^+$ B-cell progenitors within the overall compartment of $Sca1^+$ $CD117^+$ precursors in the BM of Sos1/2 DKO mice had dropped by almost 10-fold versus WT controls (Fig. 2). A more detailed analysis of the distinct B-cell maturation compartments in mice BM (e.g., $CD117^+$ $Sca1^-$ $CD19^+$ $B220^-$ IgM^- pro-B cells, $CD117^-$ $Sca1^-$ $CD19^+$ $B220^-$ IgM^- pre-B cells, $CD117^-$ $Sca1^-$ $CD19^+$ $B220^-$ IgM^+ immature B cells, and $CD117^-$ $Sca1^-$ $CD19^+$ $B220^+$ IgM^+ recirculating B cells) (Table 4) revealed that the overall drop of B-cell progenitors in Sos1/2 DKO mice was mostly due to severe reductions of pro-B (~85% to 90% reduction) and pre-B (~40% reduction) cells. Such reductions specifically occurred in animals devoid of both Sos1 and Sos2, while they were absent in the Sos1 or Sos2 single-knockout animals (Table 4). No significant changes were found in DKO animals in overall percentage of BM B cells, which could be due to the fact that both pro-B and pre-B cells accounted for only a small proportion of all BM B cells.

Changes in the relative abundances of other subpopulations of BM progenitor cells linked to the single or combined disruption of Sos1 or Sos2 were less dramatic than those described above for the B-cell progenitors. In this regard, it should be noted that the observed percent differences between single-KO animals and Sos1/2 DKO mice regarding the relative number of common myeloid precursors after 9 or 12 days of TAM treatment (Fig. 2) may be due, in part, to the more pronounced drop of B-cell progenitors observed in the Sos1/2 DKO versus single-KO mice. Since Sos1 and Sos2 single-KO mice showed similar and parallel changes in the percentages of B-cell progenitors under TAM treatment, we may rule out a preferential involvement of either isoform in causing the overall decrease in the numbers of B-cell precursors seen in the Sos1/2 DKO mice. Likewise, the rather parallel behavior of the moderate changes observed in the distributions of the BM compartments of hematopoietic stem cells from Sos1 and Sos2 single-KO animals (Fig. 2) also suggest that there is no preferential contribution made by one isoform or the other to the overall differences shown by the Sos1/2 DKO mice in comparison to WT controls.

Sos1 is the prevalent Ras-GEF during thymocyte maturation prior to T-cell receptor (TCR) signaling. BM early T-cell precursors migrate to the thymus, where they undergo a receptor-driven maturation process and ultimately become immunocompetent T cells. Because BM T-cell progenitors are not yet easily identifiable by flow cytometry, our analysis of both the early and late stages of T-cell development was fully focused on thymic maturation, from

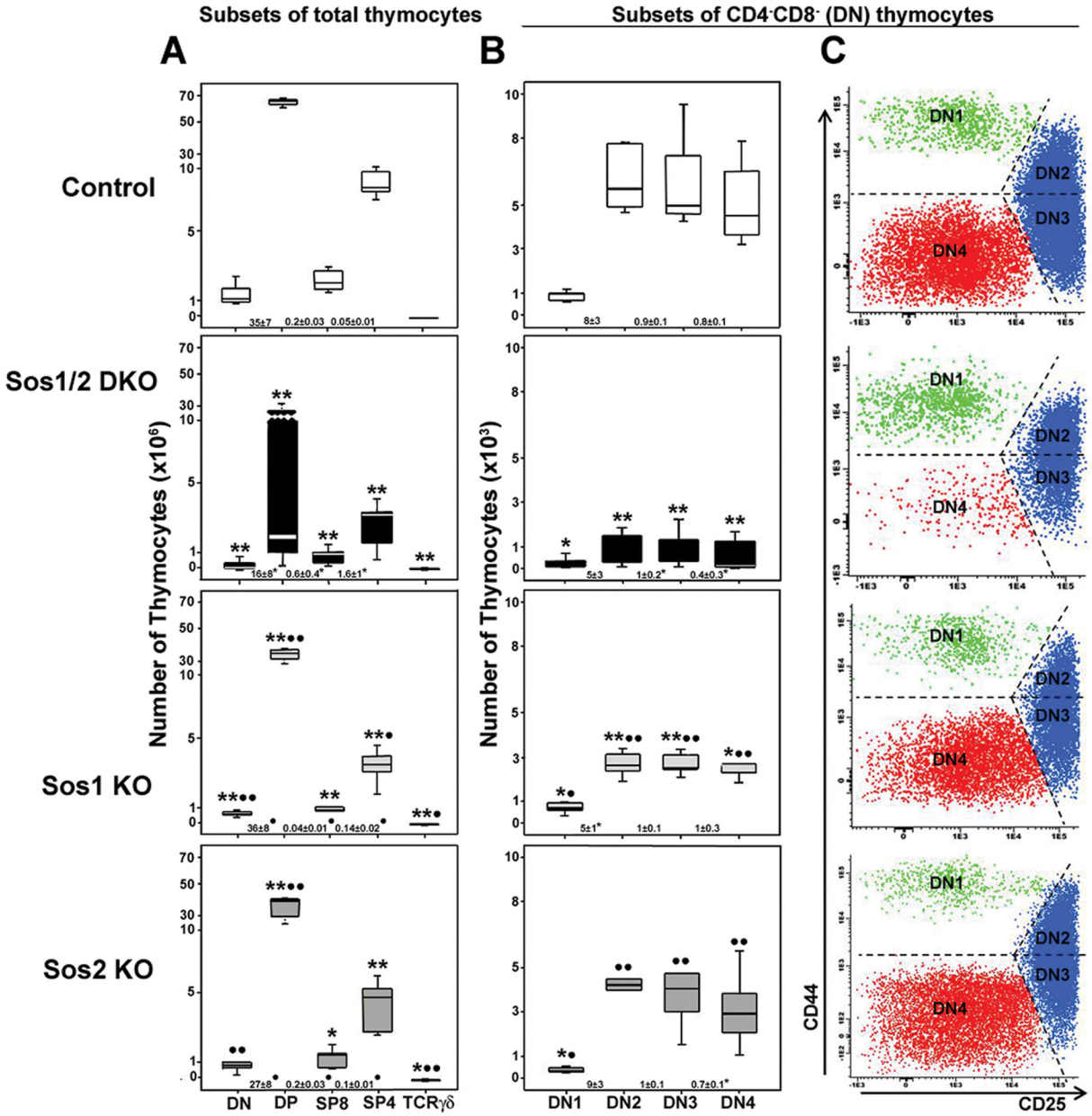

FIG 3 Effect of Sos disruption on thymocyte maturation. (A) Quantitation of CD4 CD8 double-negative (DN) thymocytes, CD4 CD8 double-positive (DP) thymocytes, CD8 single-positive cells (SP8), CD4 single-positive cells (SP4), and TCRγδ-positive T cells in the thymi of WT control mice, Sos1/2 DKO and Sos1 or Sos2 single-KO mice after 12 days of TAM treatment. Boxes extend from the 25th to the 75th percentiles. The line in the middle of each box and the vertical lines represent median values and both the 10th and 90th percentiles, respectively. (B) Distribution of DN subpopulations in the thymi of control, Sos1/2 DKO, and Sos1 or Sos2 single-KO mice after 12 days of TAM treatment. Boxes extend from the 25th to the 75th percentiles; the line in the middle and the vertical lines represent median values and both the 10th and 90th percentiles, respectively. (C) Flow cytometry dot plots gated on DN thymocytes illustrating the pattern of expression for CD44 and CD25 in the different subsets of DN thymocytes, DN1 ($CD44^+$ $CD25^-$), DN2 ($CD44^+$ $CD25^+$), DN3 ($CD44^-$ $CD25^+$), and DN4 ($CD44^-$ $CD25^-$), from mice treated with TAM for 12 days. *, $P < 0.05$ versus control mice; **, $P < 0.01$ versus control mice; ●, $P < 0.05$ versus Sos1/2 DKO mice; ●●, $P < 0.01$ versus Sos1/2 DKO mice ($n = 5$ for control and Sos1 or Sos2 single-KO mice; $n = 7$ for Sos1/2 DKO mice).

the early stages of CD4 CD8 double-negative (DN) thymocytes (DN1 to DN4) to the following more advanced stages of maturation of CD4 CD8 double-positive (DP) and CD4 or CD8 single-positive (SP) thymocytes (Fig. 3).

Overall, assessment of absolute thymocyte counts showed similar, significant reductions by 50% in Sos1 or Sos2 single-KO animals. Such decreases became much more pronounced (between 80 and 90%) in the So1/2 DKO mice (Table 5), an observation which is consistent with the loss of weight of the thymus among Sos1/2 DKO mice described above (Fig. 1). In detail, the overall number of DN cells was significantly reduced in Sos1/2 DKO and Sos1 single-KO mice in comparison to WT mice ($P = 0.004$ and $P = 0.009$, respectively). In contrast, no significant changes were detected in the number of DN thymocytes in Sos2 single-KO mice (Fig. 3; Table 5). Characterization of individual subpopulations of DN thymocytes in all four experimental groups documented a

TABLE 5 Distribution of different subsets of thymocytes and T cells in the thymi of day +12 TAM-treated control and Sos null mutant mice[a]

Subset	Mean no. of cells ± SD[b] ($\times 10^3$) from group:			
	Control	Sos1/2 DKO	Sos1 KO	Sos2 KO
Total leukocytes	78,197 ± 12,134	10,732 ± 10,600**	37,813 ± 8,177**●●	39,786 ± 14,090**●●
DN1	87.5 ± 24.2	20.7 ± 23.6*	52 ± 12*●	50 ± 12*●
DN2	713 ± 334	69.4 ± 67.1**	264 ± 55**●●	453 ± 200●●
DN3	612 ± 223	76.8 ± 75**	266 ± 50**●●	430 ± 226●●
DN4	515 ± 198	40.7 ± 62.5**	270 ± 103**●●	325 ± 180●●
DN	1,927 ± 764	207 ± 218**	874 ± 206**●●	1,258 ± 608●●
DP	62,565 ± 11,205	4,390 ± 6,662**	31,153 ± 6,450**●●	31,395 ± 11,159**●●
$CD4^-$ $CD8^+$ SP	3,061 ± 717	826 ± 438**	1,266 ± 510**	1,698 ± 706*
$CD4^+$ $CD8^-$ SP	10,350 ± 1,434	2,657 ± 1,473**	4.392 ± 1,220**●	5,247 ± 1,847**
TCRγδ$^+$ T cells	296 ± 65	56 ± 27**	143 ± 52**●	188 ± 66*●●

[a] Each subpopulation was specifically identified by flow cytometry using the following antibody mixture: CD3ε, CD4, CD5, CD8a, CD24, CD25, CD44, TCRβ, and TCRγδ. DN, CD4 CD8 double-negative thymocytes; DP, CD4 CD8 double-positive thymocytes; SP, single-positive thymocytes.

[b] *, $P < 0.05$ versus control; **, $P < 0.01$ versus control; ●, $P < 0.05$ versus Sos1/2 DKO mice; ●●, $P < 0.01$ versus Sos1/2 DKO mice ($n = 5$ for control and Sos1 or Sos2 single-KO mice; $n = 7$ for Sos1/2 DKO mice).

severe reduction of every single subpopulation of DN thymocytes (DN1 to DN4) in the Sos1/2 DKO animals versus WT controls (Fig. 3; Table 5), with a particularly significant reduction of the DN4/DN3 thymocyte ratio (Fig. 3). These results suggest the existence of a maturation blockade at pre-TCR signaling in the DKO animals. Interestingly, Sos1 single-KO mice also showed significantly reduced absolute numbers of each subset of DN thymocytes, at levels higher than those observed in the Sos1/2 DKO animals (Fig. 3; Table 5). In contrast, Sos2 single-KO mice showed normal DN thymocyte numbers for all DN subsets, with the exception of a slight reduction of DN1 cells (Fig. 3; Table 5). Since single Sos1 disruption caused a marked reduction of all DN populations, whereas depletion of Sos2 did not significantly affect these populations of thymocytes, our observation would support the notion that Sos1 is the prevalent Ras-GEF involved in the initial steps of thymocyte maturation. However, since the negative impact of Sos1 KO on DN thymocyte numbers was enhanced in the Sos1/2 DKO mice, some functional overlapping of both Sos isoforms may still occur during this process.

When assessing more-mature thymocyte subpopulations, our results showed that the absolute counts of the DP, SP, and TCRγδ$^+$ cell populations were significantly reduced in all Sos null mice versus WT mice (Fig. 3; Table 5). Such decreases were more pronounced in Sos1/2 DKO mice than in Sos1 and Sos2 single-KO mice. Sos1/2 DKO mice also showed a significantly reduced DP/DN thymocyte ratio, indicating that thymocyte expansion from the DN to the DP stage was markedly decreased in these mice versus WT controls but not in the Sos1 or Sos2 null single mutants (Fig. 3; Table 5).

T-cell numbers in secondary lymphoid tissues are altered only by simultaneous disruption of Sos1 and Sos2. After maturation, T cells leave the thymus, finding their way to secondary lymphoid tissues such as lymph nodes and the spleen through PB. To complete the phenotypic characterization of lymphoid T cells in our KO mice groups, we also evaluated the distribution of T cells in the PB and spleen from all experimental groups. Overall, our results showed highly similar patterns of distribution of total T cells and their major $CD4^+$ $CD8^-$ and $CD4^-$ $CD8^+$ subsets in the PB and spleens of single-KO and WT control mice. Conversely, Sos1/2 DKO mice showed a significant reduction (by one-half) of these T-cell populations in absolute numbers both in the spleen and in PB (Fig. 4A; Table 6).

Sos1 and Sos2 cooperation during peripheral B-cell development and homeostasis. In mice, maturing B cells leave the BM through PB and they undergo further BCR-mediated differentiation (24) to naive B cells in the spleen. Overall, no significantly different splenic B-cell counts were found in Sos1 or Sos2 single-KO mice and WT control mice. Despite this, individual mice with Sos1 or Sos2 KO genotypes displayed a statistically significant reduction of transitional type 2 B-cell (BT2) numbers versus WT animals (Fig. 4B; Table 7). In contrast, Sos1/2 DKO mice showed substantial reductions of both the overall B-cell counts and the numbers of each individual B-cell population (Fig. 4B; Table 7). Analysis of circulating B cells in the PB of Sos single-KO mice showed a pattern parallel to that found in the spleen (Fig. 4B; Table 7). In turn, Sos1/2 DKO mice showed a marked reduction of the overall number of PB B cells associated with a significant decrease of each of the different BT subpopulations of transitional B cells versus WT controls, an observation which is consistent with the depletion of B-cell production observed in the BM (Fig. 4B; Table 7).

BM transplantation assays provide mechanistic insights for the phenotypic alterations of Sos1/2 KO mice. In order to gain functional insights into the mechanisms underlying the alterations of survival/homeostasis and the developmental defects of BM progenitor cells and hematopoietic cell lineages observed in our Sos1/2 KO mice, we performed a complete set of BM transplantation assays (see Materials and Methods) involving 4 distinct combinations of receptor/donor genotypes (control/control, DKO/DKO, control/DKO, and DKO/control) (Fig. 5 and 6; Tables 8 to 11).

In this regard, we observed that engraftment of WT control BM cells into DKO recipient mice was not sufficient to rescue the animals from rapid death, as they died after around 15 days of TAM treatment, showing the same time course of death as the DKO/DKO group (data not shown). Indeed, these animals showed a similar pattern of weight loss and comparable organ/body weight ratios, for both thymus and spleen, to those found in Sos1/2 DKO mice (data not shown), indicating that defects in lymphopoietic precursors from the BM were not the primary cause of death of DKO mice. Consistent with this, transplant of BM from DKO mice into WT controls (control/DKO) did not

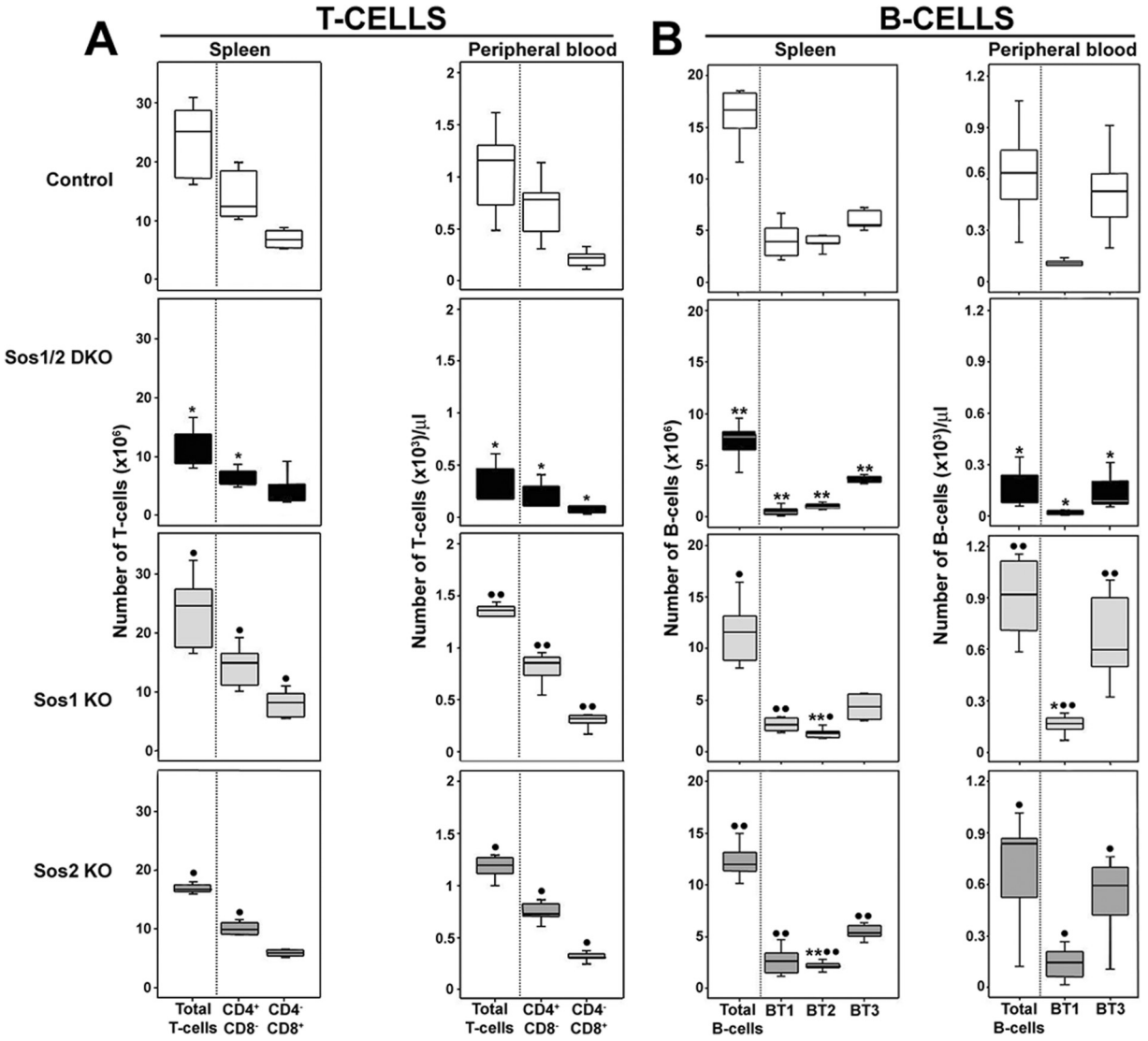

FIG 4 Effect of Sos disruption on mature T- and B-cell populations from the spleen and peripheral blood. (A) Quantitation of total T lymphocytes, $CD4^+$ $CD8^-$ and $CD4^-$ $CD8^+$ T cells isolated from the spleens and from peripheral blood from WT control, Sos1/2 DKO, and Sos1 or Sos2 single-KO mice after 12 days of TAM treatment. (B) Quantitation of total B lymphocytes and B-cell subsets in the spleens and peripheral blood from control, Sos1/2 DKO mutant, and Sos single-KO mice after 12 days of TAM treatment. Boxes extend from the 25th to the 75th percentiles; the line in the middle and the vertical lines represent median values and both the 10th and 90th percentiles, respectively. *, $P < 0.05$ versus control mice; **, $P < 0.01$ versus control mice; ●, $P < 0.05$ versus Sos1/2 DKO mice; ●●, $P < 0.01$ versus Sos1/2 DKO ($n = 5$ for control and Sos1 or Sos2 single-KO mice; $n = 7$ for Sos1/2 DKO mice). BT1 to -3, type 1 to 3 transitional B cells.

affect the overall survival rate of the recipient WT mice, and no phenotypic alterations were detected (data not shown).

Likewise, transplantation of healthy BM cells did not recover the defects of B-cell progenitors observed in the DKO mice. Thus, in line with the quantitative data shown in Tables 1 and 2, early $Sca1^+$ $CD117^+$ BM precursors in control/control transplanted animals represented around 2 to 3% of the whole BM cellularity; in contrast, the DKO/DKO transplanted mice displayed a significantly marked reduction (>50%) of the size of this pool of early $Sca1^+$ $CD117^+$ progenitors versus the control/control transplanted animals. In addition (consistent with Fig. 2), similar unchanged levels of early erythroid precursors were found among the four experimental groups (Fig. 5A). Interestingly, the percentage of common myeloid precursors (CMP) was increased in both DKO/DKO and DKO/control mice versus both control/control and control/DKO transplanted mice, and this increase was accompanied by a marked reduction in the percentage of $CD19^+$ B-cell progenitors in both the DKO/DKO and DKO/control groups (Fig. 5A). Detailed analysis of the distinct B-cell subpopulations revealed that the overall drop of this cell compartment in DKO/control and DKO/DKO transplanted mice was mostly due to a marked decrease in the percentage of pre-B cells (Table 8). In addition, the percentage of pro-B cells significantly dropped in DKO/control transplanted mice versus the control/control and control/DKO groups (Table 8). No significant changes were found in the percentages of immature BM B cells among all experimental groups versus control/control transplanted mice. In contrast, the percentage of recirculating B cells was higher in all groups than in control/control mice (Table 8). Moreover, this subset was significantly enhanced in both the DKO/control and

TABLE 6 Distribution of mature T cells in the spleens and peripheral blood of day +12 TAM-treated control and Sos null mutants

Parameter	Value (mean ± SD)[a] for mouse group:			
	Control	Sos1/2 DKO	Sos1 KO	Sos2 KO
No. of leukocytes ($\times 10^3$)	51,413 ± 16,964	20,978 ± 7,434*	39,030 ± 7,428●	32,832 ± 4,074●
No. of leukocytes/μl of PB[b]	3,347 ± 1,795	1,128 ± 889*	3,390 ± 395●	2,695 ± 984●
No. of spleen T cells ($\times 10^3$)				
Total	23,604 ± 6,674	12,563 ± 6,018*	23,819 ± 6,000●	18,110 ± 1,927●
$CD4^+$ $CD8^-$	13,992 ± 4,535	7,403,7 ± 3,319*	14,363 ± 3,432●	11,009 ± 1,621●
$CD4^-$ $CD8^+$	6,870 ± 1,651	4,462 ± 2,636	7,951 ± 2,187●	6,005 ± 592
No. of PB T cells/μl				
Total	1,060 ± 452	320 ± 206*	1,305 ± 205●●	998 ± 319●
$CD4^+$ $CD8^-$	709 ± 325	202 ± 142*	824 ± 150●●	647 ± 188●
$CD4^-$ $CD8^+$	213 ± 87	75 ± 39*	313 ± 69●●	315 ± 49●

[a] *, $P < 0.05$ versus control; ●, $P < 0.05$ versus Sos1/2 DKO mice; ●●, $P < 0.01$ versus Sos1/2 DKO mice ($n = 5$ for control and Sos1 or Sos2 single-KO mice; $n = 7$ for Sos1/2 DKO mice).
[b] PB, peripheral blood.

DKO/DKO groups compared to control/DKO mice (Table 8). These differences may be due, at least in part, to the more pronounced drop of pre-B cells observed in the first two groups.

The effects of the different BM transplantation conditions on thymocyte maturation were also examined (Fig. 5B and C; Table 9). Thus, the absolute thymocyte count showed a slight significant reduction in control/DKO transplanted mice relative to control/control mice, and the decrease was much more marked (about 75%) in both the DKO/control and DKO/DKO groups (Table 9). Regarding specific thymocyte subpopulations, the overall number of DN cells was significantly reduced in all DKO groups (control/DKO, DKO/control, and DKO/DKO) versus control/control transplanted mice. In addition, the number of DN cells in control/DKO mice was significantly higher than those detected in DKO/DKO and DKO/control groups (Fig. 5B; Table 9). Quantitation of DN thymocyte subpopulations in all four experimental transplanted groups showed reductions of every single subpopulation in control/DKO, DKO/control, and DKO/DKO transplanted mice versus the control/control group (Fig. 5C; Table 9). Interestingly, these reductions were more pronounced in both the DKO/control and DKO/DKO mice than in the control/DKO group (Fig. 5C; Table 9). As previously observed in Sos1/2 DKO animals, the DN4/DN3 ratio was significantly reduced in both the DKO/control and DKO/DKO transplanted mice with respect to the control/control and control/DKO groups (Fig. 5C).

The absolute counts of the DP thymocyte populations revealed a significant reduction in all control/DKO, DKO/control, and DKO/DKO transplanted mice versus the control/control group (Fig. 5B; Table 9). In addition, this drop was more pronounced in the DKO/control and DKO/DKO groups than in the control/DKO transplanted mice (Fig. 5B; Table 9). Interestingly, when the most mature thymocyte stages were compared, our results did not show any significant differences in the CD8 SP and CD4 SP populations among all four experimental groups (Fig. 5B; Table 9).

Finally, the distribution of mature T and B cells in the spleens and PB of our transplanted animal groups was checked (Fig. 6). Overall, our results showed no significant differences among all experimental groups regarding the total number of T cells or their main CD4 SP and CD8 SP subsets in spleens or PB (Fig. 6A; Table 10).

The total number of splenic B cells was significant lower in the control/DKO, DKO/control, and DKO/DKO groups than in

TABLE 7 Distribution of B-cell subsets in the spleens and the peripheral blood of day +12 TAM-treated control and Sos null mutant mice[a]

Parameter[b]	Value (mean ± SD)[c] for mouse group:			
	Control	Sos1/2 DKO	Sos1 KO	Sos2 KO
No. of leukocytes ($\times 10^3$)	51,413 ± 16,964	20,978 ± 7,434*	39,030 ± 7,428●	32,832 ± 4,074●
No. of leukocytes/μl PB	3,347 ± 1,795	1,128 ± 889*	3,390 ± 395●	2,695 ± 984●
No. of B cells ($\times 10^3$)				
Total B cells	17,153 ± 4,684	7,325 ± 1,742**	11,689 ± 3,061●	12,320 ± 1,768●●
BT1 ($CD19^+$ $B220^+$ IgM^{++} IgD^- $CD21^-$ $CD23^-$ $CD24^+$)	4,115 ± 1,886	481 ± 457**	2,554 ± 627●●	2,539 ± 1,361●●
BT2 ($CD19^+$ $B220^+$ IgM^{++} IgD^+ $CD21^+$ $CD23^+$ $CD24^{++}$)	4,142 ± 1,265	1,067 ± 474**	1,755 ± 483**●	2,079 ± 406**●●
BT3 ($CD19^+$ $B220^+$ IgM^+ IgD^{++} $CD21^+$ $CD23^+$ $CD24^+$)	6,025 ± 1,007	3,579 ± 977**	4,948 ± 2,419	5,421 ± 728●●
No. of PB B cells/μl				
Total B cells	634 ± 309	157 ± 128*	863 ± 682●●	682 ± 335●
BT1	94 ± 38	17 ± 15*	171 ± 74*●●	141 ± 96●
BT3	528 ± 269	134 ± 119*	657 ± 284●●	532 ± 252●

[a] Each BT subpopulation was identified by flow cytometry.
[b] BT1, -2, and -3, type 1, 2, and 3 transitional B cells; PB, peripheral blood.
[c] *, $P < 0.05$ versus control; **, $P < 0.01$ versus control; ●, $P < 0.05$ versus Sos1/2 DKO mice; ●●, $P < 0.01$ versus Sos1/2 DKO mice ($n = 5$ for control and Sos1 or Sos2 single-KO mice; $n = 7$ for Sos1/2 DKO mice).

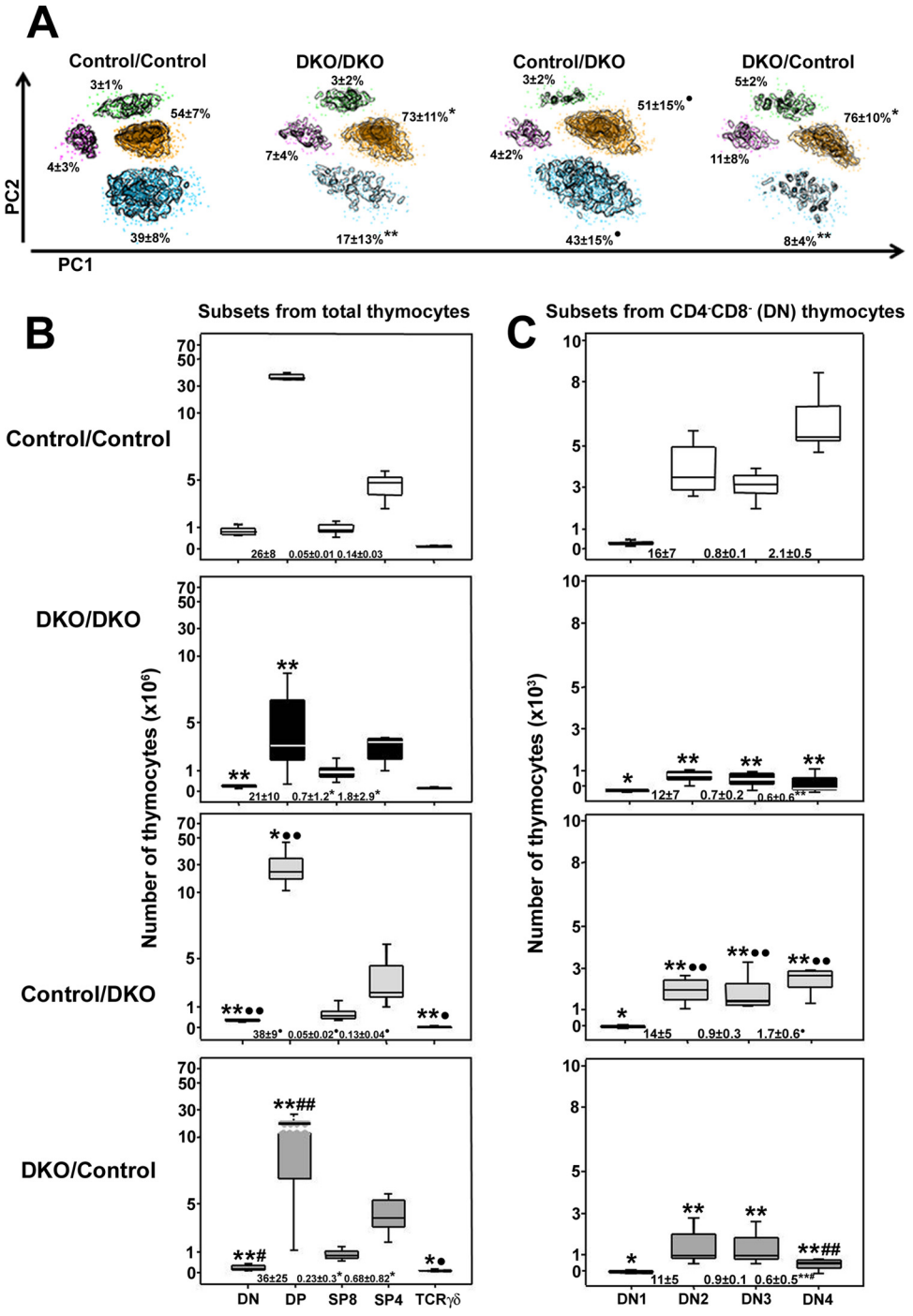

FIG 5 (A to C) Distribution of distinct subsets of Sca1$^+$ and/or CD117$^+$ progenitors and precursors cells (A), thymocytes (B), and CD4 CD8 double-negative thymocytes in the bone marrow (A) and the thymi (B and C) of transplanted mice. (A) Representative multivariate analysis (principal component analysis) density plots of different subsets of BM progenitors, including Sca1$^+$ CD117$^+$ hematopoietic stem cells (green), Sca1$^-$ CD117$^+$ CD19$^-$ TER119$^-$ common myeloid precursors (orange), Sca1$^-$ CD117$^+$ CD19$^+$ TER119$^-$ B-cell progenitors (blue), and Sca1$^-$ CD117$^+$ CD19$^-$ TER119$^+$ early erythroid precursors (pink) from the four groups of transplanted mice (transplant receptor/transplant donor: control/control, DKO/DKO, control/DKO, and DKO/control mice) 12 days after TAM feeding. The mean percentages ± SD are shown for each cell population. PC1 and -2, principal components 1 and 2. (B) Number of CD4 CD8 double-negative (DN) thymocytes, CD4 CD8 double-positive (DP) thymocytes, CD8 single-positive cells (SP8), CD4 single-positive cells (SP4), and TCRγδ-positive T cells in the thymi of control/control, DKO/DKO, control/DKO, and DKO/control mice after 12 days of TAM treatment. (C) Distribution of the different subpopulations of DN thymocytes in the thymi of control/control, DKO/DKO, control/DKO, and DKO/control mice after 12 days of TAM treatment. In panels B and C, boxes extend from the 25th to the 75th percentiles; the line in the middle and the vertical lines represent median values and both the 10th and 90th percentiles, respectively. Statistically significant differences are indicated as follows: *, $P < 0.05$ versus control/control group; **, $P < 0.01$ versus control/control group; •, $P < 0.05$ versus DKO/DKO mice; ••, $P < 0.01$ versus DKO/DKO mice; #, $P < 0.05$ versus control/DKO group; ##, $P < 0.01$ versus control/DKO group ($n = 7$ for control/control, DKO/DKO, and DKO/control mice; $n = 10$ for control/DKO mice).

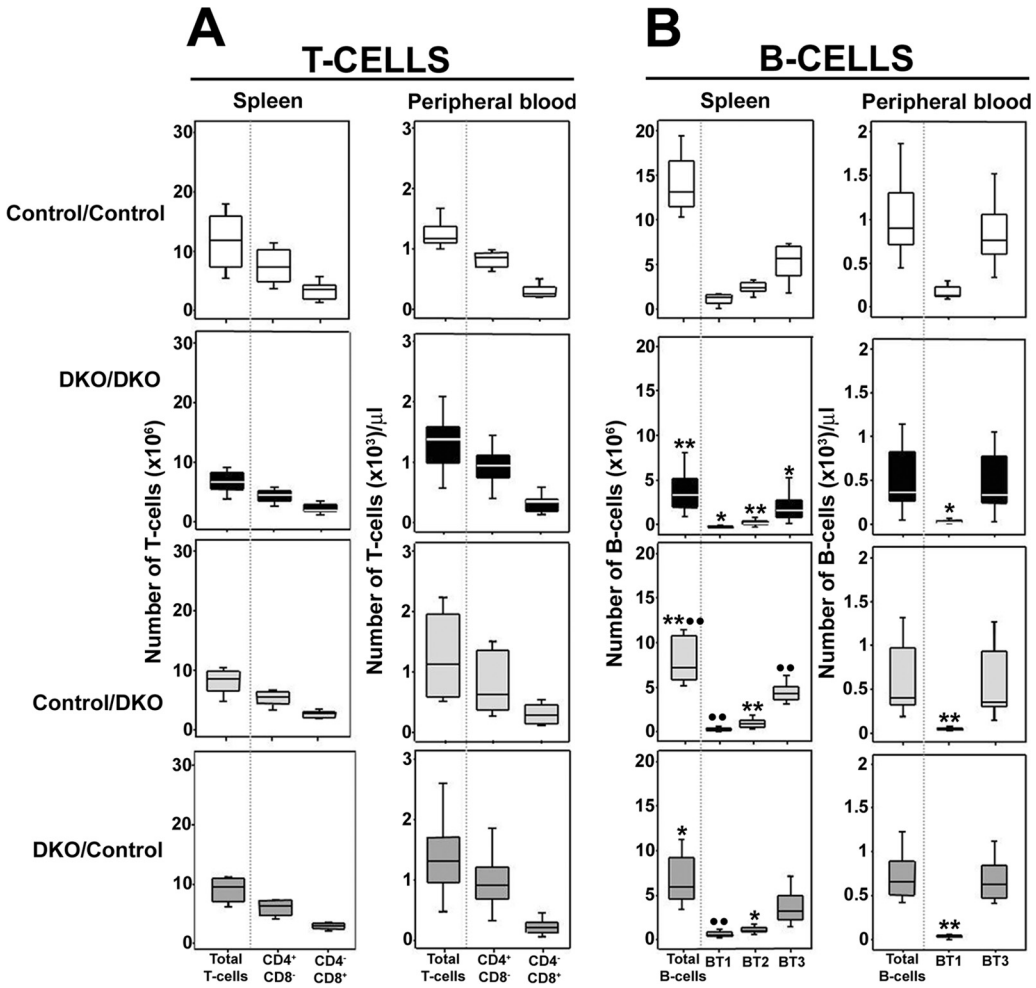

FIG 6 Effect of Sos disruption on mature T- and B-cell populations from the spleens of transplanted mice after 12 days of TAM treatment. (A) Numerical distribution of total T lymphocytes and the major $CD4^+$ $CD8^-$ and $CD4^-$ $CD8^+$ T-cell subsets isolated from the spleens and from the peripheral blood of different groups of transplanted mice (transplant receptor/transplant donor: control/control, DKO/DKO, control/DKO, and DKO/control mice). (B) Numerical distribution of total B lymphocytes and their major subsets (BT1, BT2, and BT3, type 1, 2, and 3 transitional B cells, respectively) in the spleens and the peripheral blood of the control/control, DKO/DKO, control/DKO, and DKO/control groups of transplanted mice. In both panels, boxes extend from the 25th to the 75th percentiles; the line in the middle and the vertical lines represent median values and both the 10th and 90th percentiles. Statistically significant differences are indicated as follows: *, $P < 0.05$ versus control/control group; **, $P < 0.01$ versus control/control group; ●●, $P < 0.01$ versus DKO/DKO mice; ($n = 7$ for control/control, DKO/DKO, and DKO/control mice; $n = 10$ for control/DKO mice).

the control/control mice; this reduction was more marked in the DKO/DKO mice with respect to the control/DKO group (Fig. 6B; Table 11). More-detailed analysis of splenic B-cell subsets showed that decreased B-cell numbers in all three groups were mainly attributed to the BT2 subpopulation (Fig. 6B; Table 11). In addition, the BT1 and BT3 subsets were also diminished in DKO/DKO mice versus control/control transplanted mice (Fig. 6B; Table 11); these subpopulations remained unaltered both in the control/DKO and DKO/control groups versus control/control mice (Fig. 6B and Table 11). Analysis of total circulating B cells in PB showed a slight reduction in control/DKO transplanted mice versus the control/control group (Fig. 6B; Table 11). Interestingly, the numbers of immature BT1, but not of BT3, B cells were significantly reduced in the DKO/DKO, control/DKO, and DKO/control experimental groups with respect to control/control transplanted mice (Fig. 6B; Table 11).

DISCUSSION

Here, we describe the generation and features of the first available mouse model where the functional effects of full-body expression of a Sos1 null mutation could be studied in adult animals. Previous work from our group showed that constitutive Sos1 KO mice died during midgestation whereas adult Sos2 knockout mice are viable and fertile (4, 6, 7). To overcome the embryonic lethality of Sos1 null mutation, here we produced TAM-inducible Sos1 KO mice capable of expressing the Sos1 null mutation throughout the adult body. We then bred these mice to Sos2 KO mice to generate a Sos1/2 DKO strain, which would allow direct analysis of the functional specificity versus redundancy of both isoforms of Sos in the adult organism and its tissues and cell lineages, an issue that could not be easily approached without this new animal model. Overall, our observations showed that adult animals harboring a disrupted Sos1 locus throughout the body were as viable as the

TABLE 8 Distribution of the different maturation-associated B-cell subsets in the bone marrow of transplanted groups

Maturation stage	Group	Mean % ± SD[a] on TAM treatment day +12
Pro-B cells ($CD117^+$ $Sca1^-$ $TER119^-$ $CD11b^-$ $CD19^+$ $B220^-$ IgM^-)	Control/control	6.3 ± 1.7
	DKO/DKO	6.6 ± 6.5
	Control/DKO	8.9 ± 3.2
	DKO/control	1.2 ± 0.5**#
Pre-B cells ($CD117^-$ $Sca1^-$ $TER119^-$ $CD11b^-$ $CD19^+$ $B220^-$ IgM^-)	Control/control	62.3 ± 4
	DKO/DKO	26 ± 17**
	Control/DKO	54 ± 10●●
	DKO/control	37 ± 9**##
Immature B cells ($CD117^-$ $Sca1^-$ $TER119^-$ $CD11b^-$ $CD19^+$ $B220^-$ IgM^+)	Control/control	16 ± 4
	DKO/DKO	12 ± 5
	Control/DKO	13 ± 2
	DKO/control	23 ± 8●##
Recirculating B lymphocytes ($CD117^-$ $Sca1^-$ $TER119^-$ $CD11b^-$ $CD19^+$ $B220^+$ IgM^+)	Control/control	15 ± 3
	DKO/DKO	54 ± 26**
	Control/DKO	23 ± 9*●
	DKO/control	38 ± 13●●##

[a] Values correspond to the percentages of each cell subset from all $CD19^+$ BM B cells. *, $P < 0.05$ versus control/control; **, $P < 0.01$ versus control/control mice; ●, $P < 0.05$ versus DKO/DKO mice; ●●, $P < 0.01$ versus DKO/DKO mice; #, $P < 0.05$ versus control/DKO mice; ##, $P < 0.01$ versus control/DKO mice ($n = 7$ for control/control, DKO/DKO, and DKO/control groups; $n = 10$ for control/DKO group).

constitutive Sos2 KO mice. In contrast, Sos1/2 DKO adult animals died precipitously after disruption of the Sos1 locus, indicating that expression of a single WT Sos allele, be it the Sos1 or Sos2 allele, is required and sufficient to support full animal viability and whole-body homeostasis of adult mice. Although serum blood analyses uncovered clear signs of hepatic failure in the Sos1/2 DKO mice, the exact cause of death of these animals remains unknown. The lymphopoietic defects displayed by Sos1/2 DKO animals can be excluded as the primary cause of death, as our BM transplantation assays showed that engraftment of BM from WT animals into DKO mice or from DKO into WT animals did not change in any case the original overall homeostasis and survival rates of the recipient mouse strains, indicating that Sos1/2 disruption of all the BM cell subpopulations is not enough to compromise the overall survivability of the harboring mice. Given that Ras activation and function are critical for all or most mammalian cell types, it is likely that the cause of rapid wasting and death suffered by our DKO animals is multiorgan failure, much as it happens to Ras-less mice devoid of the 3 canonical (H, N, and K) Ras proteins (25).

In any case, our data also showed that other Ras-GEFs expressed in the same animals are not able to substitute for the missing Sos proteins and support the notion that the embryonic lethality of Sos1 null mutation is due to placental malformation (6) rather than to inability to sustain progress of organism developmental programs.

Whereas Ras signaling is known to play a key role in the development and differentiation of BM progenitors (26, 27), the specific involvement of different Ras-GEFs during this process remains poorly understood. In particular, previous reports indicated that Ras-mediated effector pathways are responsible for pre-B-cell survival (28, 29), but little is known concerning the

TABLE 9 Distribution of different subsets of thymocytes and T cells in the thymi of day +12 TAM-treated engrafted mice[a]

Subset[b]	Mean no. of cells ± SD[c] ($\times 10^3$)from group:			
	Control/control	DKO/DKO	Control/DKO	DKO/control
Total leukocytes	40,483 ± 4,595	10,677 ± 9,354**	30,762 ± 12,717*●	17,379 ± 8,444**#
DN1	25.9 ± 10.5	9.9 ± 7.8*	15.3 ± 4.6*	13 ± 6.5*
DN2	385 ± 130	88.9 ± 52.7**	194 ± 52**●●	136 ± 84.9**
DN3	303 ± 68	71.3 ± 52.7**	173 ± 70**●●	128 ± 77**
DN4	605 ± 148	55 ± 75**	284 ± 130**●●	65 ± 64**##
DN	1,318 ± 307	225 ± 175**	666 ± 220**●●	342 ± 190**#
DP	32,881 ± 4,189	5,916 ± 7,130**	25,554 ± 10,791*●●	11,508 ± 6,937**##
$CD4^-$ $CD8^+$ SP	1,477 ± 423	1,247 ± 581	1,098 ± 452	1,280 ± 352
$CD4^+$ $CD8^-$ SP	4,587 ± 997	3,224 ± 1,660	3,342 ± 1,540	4,116 ± 1,306
$TCR\gamma\delta^+$ T cells	198 ± 42	56 ± 37**	97 ± 33**●	121 ± 63*●

[a] Each subpopulation was specifically identified by flow cytometry using the following antibody mixture: CD3ε, CD4, CD5, CD8a, CD24, CD25, CD44, TCRβ, and TCRγδ.
[b] DN, CD4 CD8 double-negative thymocytes; DP, CD4 CD8 double-positive thymocytes; SP, single-positive thymocytes.
[c] *, $P < 0.05$ vs control/control group; **, $P < 0.01$ versus control/control group; ●, $P < 0.05$ versus DKO/DKO group; ●●, $P < 0.01$ versus DKO/DKO group; #, $P < 0.05$ versus control/DKO group; ##, $P < 0.01$ versus control/DKO group ($n = 7$ for control/control, DKO/DKO, and DKO/control groups; $n = 10$ for control/DKO group).

TABLE 10 Distribution of mature T cells in the spleen and peripheral blood transplanted groups after 12 days of TAM treatment

Parameter	Value (mean ± SD)[a] for mouse group:			
	Control/control	DKO/DKO	Control/DKO	DKO/control
No. of leukocytes ($\times 10^3$)	29,992 ± 11,964	11,395 ± 4,403**	18,317 ± 4,713*●●	19,368 ± 11,873*
No. of leukocytes/μl of PB[b]	4,514 ± 1,734	2,713 ± 1,048*	3,122 ± 1,774	3,827 ± 1,401
No. of spleen T cells ($\times 10^3$)				
Total T cells	11,633 ± 5,079	6,402 ± 1,997	7,907 ± 1,929	9,821 ± 5,675
$CD4^+$ $CD8^-$	7,510 ± 3,179	4,000 ± 1,222	5,036 ± 1,171	6,245 ± 3,492
$CD4^-$ $CD8^+$	3,286 ± 1,575	2,087 ± 719	2,312 ± 654	2,930 ± 1,789
No. of PB T cells/μl				
Total T cells	1,284 ± 243	1,296 ± 521	1,314 ± 705	1,444 ± 707
$CD4^+$ $CD8^-$	839 ± 150	915 ± 360	861 ± 526	1,041 ± 511
$CD4^-$ $CD8^+$	308 ± 117	308 ± 159	345 ± 156	286 ± 136

[a] *, $P < 0.05$ versus control/control group; **, $P < 0.01$ versus control/control group; ●●, $P < 0.01$ versus DKO/DKO group ($n = 7$ for control/control, DKO/DKO, and DKO/control groups; $n = 10$ for control/DKO group).
[b] PB, peripheral blood.

potential participation of Sos or other Ras-GEFs during BM lymphopoiesis. Here, we showed that combined depletion of Sos1 or Sos2 resulted in a synergistic, almost complete, disappearance of B-cell progenitors, particularly pro-B cells but also pre-B cells, while individual depletion of the Sos genes did not. These results suggest that the two Sos isoforms are functionally redundant during B-cell differentiation in the BM and that no other Ras-GEFs can significantly contribute to overcoming the absence of Sos in this process.

Recent results indicate that inhibition of the Grb2-Sos interaction downregulates Raf/MEK/extracellular signal-regulated kinase (Raf/MEK/ERK) signaling and reduces HSC differentiation (30, 31). Consistent with these findings, our data also showed that individual disruption of either Sos1 or Sos2 leads to reduced percentages in the HSC compartment versus those for WT mice and also Sos1/2 DKO mice. Of note, currently available methodologies allow accurate quantitation of only the relative numbers of different BM cell subpopulations; therefore, the observed significantly higher percentage of HSC in the BM of Sos1/2 DKO mice than in that of single-KO mice most likely reflects the dramatic drop in the number of B-cell progenitors occurring in the former mice. In line with this hypothesis, no significant reduction in the percentage of the CMP was observed in single-KO or Sos1/2 DKO mice versus control mice, and, in addition, the data generated in our various BM transplantation assays for WT control and Sos1/2 DKO mice are also consistent with this notion. Altogether, these observations suggest that the Sos proteins are not essential for the development and maintenance of myeloid cells and are consistent with previous results showing that macrophage colony-stimulating factor (M-CSF)-stimulated differentiation of a murine myeloid cell line depends on persistent MEK/MAPK activation but is independent of the Grb2-Sos1 association (32).

Regarding T-cell development, here we show that Sos1 deficiency causes a significant decrease of early thymocytes at all DN stages, an observation which is consistent with previous results demonstrating a critical role for Sos1 in early T-cell development (8). Although Sos1 appears to be the prevalent player, it was also reported that Sos1 and RasGRP1 cooperate during pre-TCR-mediated T-cell development and that Sos2 is dispensable during pre-TCR-mediated and TCR-mediated positive or negative thy-

TABLE 11 Distribution of B-cell subsets in the spleen and the peripheral blood of day +12 TAM-treated control/control, DKO/DKO, control/DKO, and DKO/control groups[a]

Parameter[b]	Value (mean ± SD)[c] for mouse group:			
	Control/control	DKO/DKO	Control/DKO	DKO/control
No. of leukocytes ($\times 10^3$)	29,992 ± 11,149	11,395 ± 4,030**	18,317 ± 4,713*●●	19,368 ± 11,873*
No. of leukocytes/μl PB	4,514 ± 1,734	2,713 ± 1,048*	3,122 ± 1,774	3,827 ± 1,401
No. of B cells ($\times 10^3$)				
Total B cells	14,962 ± 5,430	4,127 ± 2,529**	7,940 ± 2,448**●●	7,625 ± 1,750*
BT1 ($CD19^+$ $B220^+$ IgM^{++} IgD^- $CD21^-$ $CD23^-$ $CD24^+$)	1,333 ± 1,106	153 ± 92*	424 ± 209●●	648 ± 376●●
BT2 ($CD19^+$ $B220^+$ IgM^{++} IgD^+ $CD21^+$ $CD23^+$ $CD24^{++}$)	2,706 ± 1,393	624 ± 344**	1,066 ± 477**	1,476 ± 1,171*
BT3 ($CD19^+$ $B220^+$ IgM^+ IgD^{++} $CD21^+$ $CD23^+$ $CD24^+$)	5,904 ± 3,530	2,379 ± 1,730*	4,741 ± 1,394●●	3,778 ± 2,211●●
No. of PB B cells/μl				
Total B cells	1,032 ± 490	538 ± 402	592 ± 395	735 ± 292
BT1	174 ± 76	36 ± 21**	39 ± 13**	45 ± 30**
BT3	845 ± 398	497 ± 378*	548 ± 393	690 ± 266

[a] Each BT subpopulation was identified by flow cytometry.
[b] BT1, -2, and -3, type 1, 2, and 3 transitional B cells; PB, peripheral blood.
[c] *, $P < 0.05$ versus control/control group; **, $P < 0.01$ versus control/control group; ●●, $P < 0.01$ versus DKO/DKO group ($n = 7$ for control/control, DKO/DKO, and DKO/control groups; $n = 10$ for control/DKO group).

mocyte development and selection (17). In this regard, our data revealed that single Sos2 disruption did not affect early maturation stages except for the DN1 subpopulation, which decreased slightly versus WT controls. A potential explanation for such a DN1 decrease might be a reduced input of T-cell progenitors arriving from the BM. Indeed, our BM transplantation assays favor this hypothesis, as they document a specific linkage between Sos1/2 disruption in the transplanted BM cells and reduction of the total number of DN thymocytes in the recipient control mice. Surprisingly, although single Sos2 disruption did not alter early thymocyte maturation, its contribution proved to be critical in the absence of Sos1, since the counts of all DN1 to -4 thymocyte populations were markedly reduced in the Sos1/2 DKO mice in comparison to the individual Sos1 or Sos2 null mutants. The apparent discrepancy concerning the marginal versus redundant role of Sos2 dispensability between our data and those previously reported by others (17) may be explained because the later studies were focused on maturation-stage-specific, Lck-CRE-mediated disruption of Sos1 occurring only at the DN2/DN3 transition, whereas in our animal model full-body disruption of the Sos1 locus occurs. The dramatic effect of double-Sos1/2 disruption on early thymocyte development could also potentially be related to alterations of progenitors arriving from the BM or dysfunction of other thymic populations involved in T-cell development such as dendritic cells. In this regard, BM cells from Sos1/2 DKO mice caused disruption of early thymocyte development stages after engraftment into control mice, and, additionally, healthy BM cells engrafted into Sos1/2 DKO mice did not palliate the defects in early thymocyte development. Altogether, these results suggest that the severe effect of early thymocyte development linked to concomitant Sos1/2 deficiency is a consequence, at least in part, of (i) reduced arrival/input of cells from the BM and (ii) impaired DN maturation at pre-TCR signaling.

Previous reports indicate that, as thymocyte maturation progresses, Sos involvement decays and RasGRP1 function becomes prevalent at the level of TCR-mediated signaling (8, 14, 16, 33, 34), although a recent study also reported functional cooperation between Sos1 and RasGRP1 during negative thymic selection (17). Consistently, our results showed that the cellular expansion taking place during the transition from DN to DP thymocytes was markedly reduced in Sos1/2 double-null mutants but not in mice lacking only one Sos isoform; such results support the notion of functional redundancy between Sos1 and Sos2 to sustain expansion of thymocytes occurring during progress through these maturation stages. Most interestingly, our results also showed that Sos1/2 DKO was associated with a marked decrease in the absolute number of T cells and their major $CD4^+$ $CD8^-$ and $CD4^-$ $CD8^+$ subsets both in PB and the spleen, whereas single Sos1 or Sos2 disruption did not alter mature T-cell counts in both tissues. Such observations further point out the potential overlapping role of the Sos isoforms during the latter stages of T-cell development, although they could also be a consequence of the disruption or early thymocyte maturation occurring in the DKO mice. The data from our present BM transplantation experiments, together with the recent demonstration of Sos-independent, TCR-mediated Erk activation in peripheral human T cells (35), favor the second possibility, although a more definitive mechanistic answer requires further investigations.

Similarly, analysis of the distribution of maturation-associated B-cell subsets in the spleen and PB also showed that only combined disruption of the two Sos proteins leads to a clear alteration of all subsets of mature B lymphocytes but marginal-zone B cells, except for slightly decreased BT2 counts in the spleens of Sos1 and Sos2 single-KO mice. Since previous reports in which Erk activation during BCR-mediated B-cell maturation is analyzed support a prevalent role in this process for RasGRP1/2 versus Sos (12, 14), we speculate that the significantly reduced numbers of B cells detected in the PB and spleens of Sos1/2 DKO mutants are mainly a consequence of the dramatic drop in B-cell production in the BM rather than an alteration of more-mature B-cell populations. However, simultaneous occurrence of an altered homeostasis of mature B cells cannot be completely ruled out, particularly because an increased rate of apoptosis in association with a significant disruption of normal spleen histology was also observed.

In summary, here we described the first mouse model where, to our knowledge, the effect of full-body expression of a Sos1 null mutation could be studied during adulthood. Our data demonstrate functional redundancy of Sos1 and Sos2 for homeostasis and survival of the full organism and for the development and maturation of B and T lymphoid cells. Ascertaining the functional properties of the Sos family members is relevant for physiological and pathological processes in view of their role as universal GEF activators in multiple Ras-mediated signaling pathways.

ACKNOWLEDGMENTS

Work was supported by grants FIS-PS09/01979, RTICC-RD12/0036/0001, and RD12/0036/0048 from Instituto de Salud Carlos III (Madrid, Spain) and Fundación Samuel Solórzano (Salamanca, Spain). This research was also supported by the Intramural Research Program of the CCR, NCI, NIH.

Nuria Calzada, Ximena Bonilla, and Javier Borrajo are gratefully acknowledged for technical assistance.

REFERENCES

1. **Buday L, Downward J.** 2008. Many faces of Ras activation. Biochim. Biophys. Acta **1786:**178–187.
2. **Karnoub AE, Weinberg RA.** 2008. Ras oncogenes: split personalities. Nat. Rev. Mol. Cell Biol. **9:**517–531.
3. **Castellano E, Santos E.** 2011. Functional specificity of ras isoforms: so similar but so different. Genes Cancer **2:**216–231.
4. **Rojas JM, Oliva JL, Santos E.** 2011. Mammalian son of sevenless guanine nucleotide exchange factors: old concepts and new perspectives. Genes Cancer **2:**298–305.
5. **Cherfils J, Zeghouf M.** 2013. Regulation of small GTPases by GEFs, GAPs, and GDIs. Physiol. Rev. **93:**269–309.
6. **Qian X, Esteban L, Vass WC, Upadhyaya C, Papageorge AG, Yienger K, Ward JM, Lowy DR, Santos E.** 2000. The Sos1 and Sos2 Ras-specific exchange factors: differences in placental expression and signaling properties. EMBO J. **19:**642–654.
7. **Esteban LM, Fernandez-Medarde A, Lopez E, Yienger K, Guerrero C, Ward JM, Tessarollo L, Santos E.** 2000. Ras-guanine nucleotide exchange factor sos2 is dispensable for mouse growth and development. Mol. Cell. Biol. **20:**6410–6413.
8. **Kortum RL, Sommers CL, Alexander CP, Pinski JM, Li W, Grinberg A, Lee J, Love PE, Samelson LE.** 2011. Targeted Sos1 deletion reveals its critical role in early T-cell development. Proc. Natl. Acad. Sci. U. S. A. **108:**12407–12412.
9. **Steelman LS, Franklin RA, Abrams SL, Chappell W, Kempf CR, Bäsecke J, Stivala F, Donia M, Fagone P, Nicoletti F, Libra M, Ruvolo P, Ruvolo V, Evangelisti C, Martelli AM, McCubrey JA.** 2011. Roles of the Ras/Raf/MEK/ERK pathway in leukemia therapy. Leukemia **25:**1080–1094.
10. **Kurosaki T.** 2002. Regulation of B cell fates by BCR signaling components. Curr. Opin. Immunol. **14:**341–347.
11. **Niiro H, Clark EA.** 2002. Regulation of B-cell fate by antigen-receptor signals. Nat. Rev. Immunol. **2:**945–956.

12. **Oh-hora M, Johmura S, Hashimoto A, Hikida M, Kurosaki T.** 2003. Requirement for Ras guanine nucleotide releasing protein 3 in coupling phospholipase C-gamma2 to Ras in B cell receptor signaling. J. Exp. Med. **198:**1841–1851.
13. **Li LX, Goetz CA, Katerndahl CD, Sakaguchi N, Farrar MA.** 2010. A Flt3- and Ras-dependent pathway primes B cell development by inducing a state of IL-7 responsiveness. J. Immunol. **184:**1728–1736.
14. **Roose JP, Mollenauer M, Ho M, Kurosaki T, Weiss A.** 2007. Unusual interplay of two types of Ras activators, RasGRP and SOS, establishes sensitive and robust Ras activation in lymphocytes. Mol. Cell. Biol. **27:** 2732–2745.
15. **Das J, Ho M, Zikherman J, Govern C, Yang M, Weiss A, Chakraborty AK, Roose JP.** 2009. Digital signaling and hysteresis characterize ras activation in lymphoid cells. Cell **136:**337–351.
16. **Dower NA, Stang SL, Bottorff DA, Ebinu JO, Dickie P, Ostergaard HL, Stone JC.** 2000. RasGRP is essential for mouse thymocyte differentiation and TCR signaling. Nat. Immunol. **1:**317–321.
17. **Kortum RL, Sommers CL, Pinski JM, Alexander CP, Merrill RK, Li W, Love PE, Samelson LE.** 2012. Deconstructing Ras signaling in the thymus. Mol. Cell. Biol. **32:**2748–2759.
18. **Kratz CP, Niemeyer CM, Thomas C, Bauhuber S, Matejas V, Bergsträsser E, Flotho C, Flores NJ, Haas O, Hasle H, van den Heuvel-Eibrink MM, Kucherlapati RS, Lang P, Roberts AE, Starý J, Strahm B, Swanson KD, Trebo M, Zecca M, Neel B, Locatelli F, Loh ML, Zenker M.** 2007. Mutation analysis of Son of Sevenless in juvenile myelomonocytic leukemia. Leukemia **21:**1108–1109.
19. **Hasle H.** 2009. Malignant diseases in Noonan syndrome and related disorders. Horm. Res. **2:**8–14.
20. **Baltanas FC, Casafont I, Weruaga E, Alonso JR, Berciano MT, Lafarga M.** 2011. Nucleolar disruption and cajal body disassembly are nuclear hallmarks of DNA damage-induced neurodegeneration in Purkinje cells. Brain Pathol. **21:**374–388.
21. **Castellano E, Guerrero C, Nunez A, De Las Rivas J, Santos E.** 2009. Serum-dependent transcriptional networks identify distinct functional roles for H-Ras and N-Ras during initial stages of the cell cycle. Genome Biol. **10:**R123. doi:10.1186/gb-2009-10-11-r123.
22. **Recio JS, Alvarez-Dolado M, Diaz D, Baltanas FC, Piquer-Gil M, Alonso JR, Weruaga E.** 2011. Bone marrow contributes simultaneously to different neural types in the central nervous system through different mechanisms of plasticity. Cell Transplant. **20:**1179–1192.
23. **Matarraz S, Lopez A, Barrena S, Fernandez C, Jensen E, Flores J, Bárcena P, Rasillo A, Sayagues JM, Sánchez ML, Hernandez-Campo P, Hernandez Rivas JM, Salvador C, Fernandez-Mosteirín N, Giralt M, Perdiguer L, Orfao A.** 2008. The immunophenotype of different immature, myeloid and B-cell lineage-committed CD34+ hematopoietic cells allows discrimination between normal/reactive and myelodysplastic syndrome precursors. Leukemia **22:**1175–1183.
24. **Allman D, Srivastava B, Lindsley RC.** 2004. Alternative routes to maturity: branch points and pathways for generating follicular and marginal zone B cells. Immunol. Rev. **197:**147–160.
25. **Drosten M, Dhawahir A, Sum EY, Urosevic J, Lechuga CG, Esteban LM, Castellano E, Guerra C, Santos E, Barbacid M.** 2010. Genetic analysis of Ras signalling pathways in cell proliferation, migration and survival. EMBO J. **29:**1091–1104.
26. **Khalaf WF, White H, Wenning MJ, Orazi A, Kapur R, Ingram DA.** 2005. K-Ras is essential for normal fetal liver erythropoiesis. Blood **105:** 3538–3541.
27. **Odai H, Hanazono Y, Sasaki K, Iwamatu A, Yazaki Y, Hirai H.** 1997. The signal transduction through Grb2/Ash in hematopoietic cells. Leukemia **11**(Suppl 3)**:**405–407.
28. **Iritani BM, Forbush KA, Farrar MA, Perlmutter RM.** 1997. Control of B cell development by Ras-mediated activation of Raf. EMBO J. **16:**7019–7031.
29. **Nagaoka H, Takahashi Y, Hayashi R, Nakamura T, Ishii K, Matsuda J, Ogura A, Shirakata Y, Karasuyama H, Sudo T, Nishikawa S, Tsubata T, Mizuochi T, Asano T, Sakano H, Takemori T.** 2000. Ras mediates effector pathways responsible for pre-B cell survival, which is essential for the developmental progression to the late pre-B cell stage. J. Exp. Med. **192:**171–182.
30. **Kumkhaek C, Aerbajinai W, Liu W, Zhu J, Uchida N, Kurlander R, Hsieh MM, Tisdale JF, Rodgers GP.** 2013. MASL1 induces erythroid differentiation in human erythropoietin-dependent CD34+ cells through the Raf/MEK/ERK pathway. Blood **121:**3216–3227.
31. **Modi H, Li L, Chu S, Rossi J, Yee JK, Bhatia R.** 2011. Inhibition of Grb2 expression demonstrates an important role in BCR-ABL-mediated MAPK activation and transformation of primary human hematopoietic cells. Leukemia **25:**305–312.
32. **Gobert Gosse S, Bourgin C, Liu WQ, Garbay C, Mouchiroud G.** 2005. M-CSF stimulated differentiation requires persistent MEK activity and MAPK phosphorylation independent of Grb2-Sos association and phosphatidylinositol 3-kinase activity. Cell. Signal **17:**1352–1362.
33. **Roose JP, Mollenauer M, Gupta VA, Stone J, Weiss A.** 2005. A diacylglycerol-protein kinase C-RasGRP1 pathway directs Ras activation upon antigen receptor stimulation of T cells. Mol. Cell. Biol. **25:**4426–4441.
34. **Oki T, Kitaura J, Watanabe-Okochi N, Nishimura K, Maehara A, Uchida T, Komeno Y, Nakahara F, Harada Y, Sonoki T, Harada H, Kitamura T.** 2012. Aberrant expression of RasGRP1 cooperates with gain-of-function NOTCH1 mutations in T-cell leukemogenesis. Leukemia **26:** 1038–1045.
35. **Warnecke N, Poltorak M, Kowtharapu BS, Arndt B, Stone JC, Schraven B, Simeoni L.** 2012. TCR-mediated Erk activation does not depend on Sos and Grb2 in peripheral human T cells. EMBO Rep. **13:**386–391.